Published in final edited form as:

J Pharm Sci. 2016 February ; 105(2): 443–459. doi:10.1016/j.xphs.2015.11.008.

Sandwich-Cultured Hepatocytes as a Tool to Study Drug Disposition and Drug-Induced Liver Injury

KYUNGHEE YANG[1,*], **CEN GUO**[2,*], **JEFFREY L WOODHEAD**[1], **ROBERT LST. CLAIRE III**[3], **PAUL B WATKINS**[1,2], **SCOTT Q SILER**[1], **BRETT A HOWELL**[1], and **KIM LR BROUWER**[2]

[1]The Hamner-UNC Institute for Drug Safety Sciences, The Hamner Institutes for Health Sciences, Research Triangle Park, NC 27709

[2]Division of Pharmacotherapy and Experimental Therapeutics, UNC Eshelman School of Pharmacy, The University of North Carolina at Chapel Hill, Chapel Hill, NC 27599

[3]Qualyst Transporter Solutions, LLC, Durham, NC 27713

Abstract

Sandwich-cultured hepatocytes (SCH) are metabolically competent and have proper localization of basolateral and canalicular transporters with functional bile networks. Therefore, this cellular model is a unique tool that can be used to estimate biliary excretion of compounds. SCH have been used widely to assess hepatobiliary disposition of endogenous and exogenous compounds and metabolites. Mechanistic modeling based on SCH data enables estimation of metabolic and transporter-mediated clearances, which can be employed to construct physiologically-based pharmacokinetic models for prediction of drug disposition and drug-drug interactions in humans. In addition to pharmacokinetic studies, SCH also have been employed to study cytotoxicity and perturbation of biological processes by drugs and hepatically-generated metabolites. Human SCH can provide mechanistic insights underlying clinical drug-induced liver injury (DILI). In addition, data generated in SCH can be integrated into systems pharmacology models to predict potential DILI in humans. In this review, applications of SCH in studying hepatobiliary drug disposition and bile acid-mediated DILI are discussed. An example is presented to show how data generated in the SCH model was used to establish a quantitative relationship between intracellular bile acids and cytotoxicity, and how this information was incorporated into a systems pharmacology model for DILI prediction.

Corresponding author: Kim L.R. Brouwer, Current address: UNC Eshelman School of Pharmacy, The University of North Carolina at Chapel Hill, 311, Pharmacy Lane CB #7569 Kerr Hall, Chapel Hill, NC 27599-7569, ; Email: kbrouwer@unc.edu, Telephone: 1 – 919 – 962 – 7030, Fax: 1 – 919 – 962 – 0644

*Authors contributed equally.

CONFLICT OF INTEREST

Dr. Kim Brouwer is co-inventor of the sandwich-cultured hepatocyte technology for quantification of biliary excretion (B-CLEAR®) and related technologies, which have been licensed exclusively to Qualyst Transporter Solutions. Drs. Kyunghee Yang, Jeffrey L Woodhead, Scott Q Siler, and Brett A Howell are employees of DILIsym Services Inc., a company who licenses the DILIsym® software for commercial use. Drs. Kyunghee Yang, Jeffrey L Woodhead, Scott Q Siler, Brett A Howell Paul B. Watkins have equity positions in DILIsym Services Inc.

Keywords

Sandwich-cultured hepatocytes (SCH); hepatic clearance; hepatobiliary disposition; bile acid transporters; toxicity; mathematical models

INTRODUCTION

The liver is one of the major organs responsible for the metabolism and excretion of endogenous and exogenous molecules. Among many in vitro and in vivo model systems, primary hepatocytes remain the gold standard to assess hepatic drug metabolism and transport. Hepatocytes can be isolated from the species of interest, including humans, to address species differences in hepatic disposition of drugs. Primary hepatocytes express multiple metabolic enzymes and transporters, enabling assessment of overall hepatobiliary drug disposition. However, hepatocytes in suspension or under conventional culture conditions quickly lose cell polarity and viability, which limits their utility.[1,2] Culturing hepatocytes between two layers of gelled collagen (sandwich configuration) improves morphology and viability of hepatocytes, and maintains function for longer periods of time in culture.[3,4] In addition, sandwich-cultured hepatocytes (SCH) regain polarity, allowing proper localization of basolateral and canalicular transporters as well as formation of functional bile networks (Figure 1).[5,6]

When properly cultured, the expression and function of basolateral uptake transporters including sodium taurocholate co-transporting polypeptide (NTCP) and organic anion transporting polypeptides (OATPs) are maintained over time in human SCH,[7–9] whereas down-regulation of Ntcp and Oatp has been reported for rat SCH.[6,7] Upon isolation, hepatocytes lose biliary excretory function due to internalization of canalicular efflux transporters.[10] However, canalicular transport proteins [e.g, bile salt export pump (BSEP/Bsep), P-glycoprotein (P-gp), breast cancer resistance protein (BCRP/Bcrp), and multidrug resistance-associated protein (MRP/Mrp) 2] properly localize over time and regain excretory function in human and rat SCH.[50] A schematic representation of hepatic transporters in SCH is shown in Figure 1. Phase I [i.e., cytochrome P450 (CYP)] and phase II [e.g., UDP-glucuronosyltransferase (UGT), sulfotransferase (SULT)] metabolizing enzymes also are expressed in SCH, although some enzymes exhibit decreased expression and/or function over time in SCH compared to freshly isolated hepatocytes, depending on the culture conditions and medium composition.[12–14] The influence of culture conditions and culture time on the expression and/or function of enzymes and transporters in the SCH system have been reviewed in detail elsewhere and are not the main focus of this manuscript.[1,15,16]

SCH provide a unique tool to estimate biliary excretion of compounds. Substances excreted into bile and accumulated in the canalicular network can be quantified by modulating tight junctions using buffer with and without calcium.[17,18] Therefore, SCH have been used widely to assess hepatobiliary disposition of drugs and metabolites, and potential drug-drug interactions (DDIs). Transcriptional and post-translational regulatory machinery are well-maintained in SCH, which makes it a suitable model for studying induction and feedback regulation of enzymes and transporters in response to compounds or other interventions.[4,19]

SCH that express functional metabolic enzymes also have been employed to study the pharmacology and toxicology of drugs and hepatically-generated metabolites. Because of the essential role of the liver in drug elimination, it is often a target organ of drug-induced toxicity. SCH have been used in the assessment of direct cytotoxicity and in mechanistic studies to determine perturbations of biological processes and to better understand underlying mechanisms of drug-induced liver injury (DILI).

In this manuscript, applications of SCH in studying hepatobiliary drug disposition and DILI are reviewed. First, use of the SCH system to characterize hepatic drug metabolism and transport is discussed. Predictions of in vivo drug disposition and clinical DDIs using SCH data combined with mechanistic and/or physiologically-based pharmacokinetic (PBPK) modeling also are reviewed. The use of SCH to study mechanisms underlying DILI is discussed with a focus on bile acid-drug interactions with hepatic transporters. An example of how SCH data can be used to develop a systems pharmacology model of DILI to predict clinical hepatotoxicity is introduced.

USE OF SANDWICH–CULTURED HEPATOCYTES IN STUDYING DRUG DISPOSITION

During drug discovery and development, assessment of metabolism and transport of new chemical entities is important to predict clinical exposure and potential DDIs. In this section, the use of SCH to study drug disposition is reviewed with a focus on metabolism and hepatobiliary transport of compounds and DDIs, and enzyme-transporter interplay. This section also highlights the estimation of enzyme- and transporter-mediated intrinsic clearance values using mechanistic pharmacokinetic modeling in addition to empirical methods. In vitro-in vivo extrapolation of intrinsic clearance and incorporation into PBPK modeling is discussed.

Metabolism

SCH have been used to study drug disposition, including hepatic uptake, metabolism and biliary excretion. Although human liver microsomes (HLMs), S9 subcellular fractions, and primary hepatocytes cultured in monolayers (without extracellular matrix overlay) are commonly used in metabolism studies of drugs and endogenous substrates, SCH are often used when extended incubation times (>24 hr) are needed, after which the viability and function of primary hepatocytes cultured in monolayers begin to deteriorate[1]. To demonstrate the applicability of SCH in predicting drug metabolism after extended exposure, the metabolic clearance values of low clearance drugs tolbutamide and warfarin, as well as a high clearance compound 7-ethoxycoumarin, were estimated using mathematical modeling after co-incubation with human SCH for 48 hr.[20,21] The calculated intrinsic clearance was in accordance with literature reports. Another advantage of using SCH in drug metabolism studies is the presence of non-microsomal reductive enzymes, as demonstrated in a study of DB829. DB829, the active metabolite of an antitrypanosomal prodrug, was detected only in trace amounts in HLMs at the end of the 180-min incubation, but was detected readily in human SCH throughout the 24-hr incubation.[22]

Metabolism-Mediated DDIs—Both inhibition- and induction-mediated DDIs have been studied using SCH. The CYP substrates used in these studies generally penetrate the hepatocytes via passive diffusion to eliminate the confounding effect of transporters. Although CYP inhibition has been studied primarily using HLMs, a few studies using SCH have been reported. The inhibitory effect of tritolide on CYP3A was evaluated by Shen et al.[23] Both the expression and activity (measured by midazolam hydroxylation) of CYP3A in rat SCH were reduced after exposure to tritolide for up to 24 hr. Bi et al. [24] reported that the intracellular accumulation of buprenorphine and midazolam in human SCH was increased by rifamycin SV due to inhibition of CYP3A4 and UGT1A1, which mediate the metabolism of these two victim substrates. SCH allow for longer exposure time, making them suitable for CYP induction studies. For example, the activity of CYP3A was assessed in human SCH after incubation with pregnancy-related hormones for 72 hr.[25]

Hepatobiliary Transport

Mechanisms of Hepatobiliary Disposition—Under appropriate culture conditions, SCH express key transport proteins that are properly localized, and therefore, they are uniquely advantageous to study the mechanisms of hepatobiliary transport of a compound as well as the effects of a compound on hepatobiliary transporters. SCH isolated from naturally occurring genetically deficient rodents [e.g., Mrp2-deficient Wistar rats (TR^- rats), Eisai-hyperbilirubinemic Sprague-Dawley rats (EHBR rats)] or genetically modified animals with loss-of-function of a specific transporter can be used to elucidate the role of that transporter in the disposition of a compound.[26,27] Knockdown of Bcrp using RNA interference in SCH isolated from wild-type rats elucidated the role of Bcrp in drug hepatobiliary disposition.[28,29] With human SCH, the role of individual transporters can be determined by using “specific” transporter inhibitors or by modifying the experimental conditions. For example, the role of NTCP could be assessed by measuring uptake in the absence and presence of sodium. However, highly specific transport inhibitors and substrates are lacking, and genetically modified animals are only limited to a few transporters. Therefore, a multi-experimental approach integrating SCH data, transfected systems and membrane vesicles can be used to characterize the involvement of multiple transporters.[26,27] Understanding the transport mechanism(s) could facilitate identification of potential DDIs involving uptake and efflux transporters. Previous reviews have shown the utility of SCH for these applications,[1,15] and recent reports are discussed below. A focused discussion about drug effects on bile acid disposition is in the following section “Mechanistic Investigations of Bile Acid-Mediated DILI”.

Yanni et al. identified the hepatic transporters involved in micafungin disposition by co-incubation of micafungin with an NTCP inhibitor [taurocholic acid (TCA)], an OATP inhibitor (rifampin), BSEP inhibitors (TCA and nefazodone), a mixed P-gp/BCRP inhibitor (GF120918), as well as a P-gp and MRP2 inhibitor (cyclosporine A).[31] Mohamed et al. reported that the disposition of tacrine, which was approved for treatment of Alzheimer’s disease, was mediated by Octs, Mrp2 and P-gp by using rat SCH and chemical inhibitors.[32] A similar approach to elucidate the responsible hepatobiliary transporters for 17α-hydroxyprogesterone caproate and its effect on bile acid transporters has been reported.[33] One caveat with this type of approach is that these “specific” inhibitors may have other

effects on metabolism and/or transport. To overcome this issue, transporter assays using transfected cells can be used to confirm findings from the SCH studies. For example, disposition of a natural product timosaponin b2 (TB2) was characterized using rat SCH and involvement of specific transporters was confirmed using human OATP1B1- and OATP1B3-expressing HEK-293 cells and membrane vesicles isolated from cells expressing human MRP2 and BCRP.[34]

In addition to drugs, the disposition of endogenous compounds has been studied using SCH. For example, amyloid-β (Aβ) hepatic disposition was studied in human SCH since Aβ accumulation contributes to Alzheimer's disease.[35] Aβ was found to be taken up primarily by low-density lipoprotein receptor-related protein-1 (LRP1), and effluxed by P-gp. This finding indicates that enhancement of Aβ hepatic clearance via LRP1 and P-gp induction could be a novel therapeutic approach for the prevention and treatment of Alzheimer's disease. Toxic compounds such as arsenic also have been studied in human SCH. The results suggest that arsenic basolateral efflux prevails over biliary excretion, and is mediated at least in part by MRPs, most likely MRP4.[36]

Estimation of Transport Clearance—In the estimation of uptake clearance, hepatocytes in suspension generally are preferred due to the ease of use [37,38] and concerns regarding down-regulation of uptake transporters in rat SCH.[7] However, uptake transporter function in human SCH remains similar to freshly isolated hepatocytes under appropriate culture conditions.[6,7] Recent evidence suggests that cryopreserved hepatocytes cultured in sandwich configuration are a more feasible research tool to evaluate in vitro transport parameters without the negative impact derived from membrane leakage during cryopreservation.[9] To distinguish active uptake from passive diffusion, hepatocytes can be co-incubated with an OATP inhibitor if the active uptake is mediated mainly by OATP. For example, rifampicin SV (100 μM) was reported to block OATP function in OATP-transfected cell lines and human SCH without affecting the passive diffusion.[24,39] Alternatively, active uptake in SCH can be determined by the difference in uptake in the absence and presence of sodium if the active uptake is governed primarily by NTCP. Active uptake also may be differentiated from passive diffusion by comparing the difference in uptake determined at 37°C and 4°C. However, reduced uptake at 4°C might be an artificial effect of a more rigid cell membrane, and thus, active uptake using this approach may be over-estimated.[40]

In SCH, the biliary efflux clearance and biliary excretion index (BEI) can be calculated using B-CLEAR® technology and Equations 1–3.[41] A detailed description of B-CLEAR® technology, including an overview of the advantages and limitations has been published by Swift et al.[1] Essentially, the accumulation of compound in cells + bile canaliculi and the accumulation of compound in cells can be differentiated by modulating the tight junctions using Ca^{2+}-containing and Ca^{2+}-free Hank's balanced salt solution (HBSS). The utility of SCH data for extrapolation from in vitro biliary clearance to in vivo biliary clearance was reviewed previously by De Bruyn et al.[15]

$$CL_{b,app,in\ vitro} = \frac{Amount_{cell+bile} - Amount_{cell}}{Time \times Concentration_{medium}} \quad \text{Eq. 1}$$

$$CL_{b,int,in\ vitro} = \frac{Amount_{cell+bile} - Amount_{cell}}{Time \times Concentration_{cell}} \quad \text{Eq. 2}$$

$$BEI = \frac{Amount_{cell+bile} - Amount_{cell}}{Amount_{cell+bile}} \times 100\% \quad \text{Eq. 3}$$

$CL_{b,\ app,\ in\ vitro}$ and $CL_{b,\ int,\ in\ vitro}$ represent in vitro apparent biliary clearance and in vitro intrinsic biliary clearance, respectively. BEI represents biliary excretion index, which is the fraction of compound accumulated in the bile compartment relative to the total accumulation in cells plus bile.

Use of the SCH assay to categorize compounds as low, intermediate or high biliary clearance was first reported by Liu et al[41], and has been confirmed by numerous investigators and reviewed by De Bruyn et al. [15] and Swift et al.[1] Pan et al.[42] evaluated the biliary clearance of 110 compounds from Novartis exhibiting different permeability properties using the rat SCH model. The predicted biliary clearance from rat SCH correlated well with in vivo rat data, except for underestimation of biliary clearance for compounds with extremely low passive permeability and metabolism. The rank order of biliary clearance from human SCH data corresponded with clinical data for compounds with low to high biliary clearance,[43] despite slight underestimation of the absolute values (by 50–80%). The underestimation might be due to the decreased activity of uptake transporters depending on the culture conditions, and use of compound concentrations in the medium (Eq.1) instead of the intracellular concentrations (Eq.2) to predict biliary clearance. More accurate estimates of biliary clearance parameters for in vitro-in vivo scaling are discussed in greater detail in the “Mechanistic and PBPK Modeling” section.

To improve the accuracy of biliary clearance predictions using both rat and human SCH, the following approaches have been reported. The correlation between in vitro and in vivo biliary clearance is improved by using unbound plasma concentrations in the estimation of in vivo biliary clearance.[44] Moreover, the difference between in vivo intrinsic biliary clearance and predicted intrinsic biliary clearance from the SCH data using Eq. 2 is smaller than the difference between in vivo apparent biliary clearance and predicted apparent biliary clearance from SCH data based on Eq. 1.[45] Therefore, in vitro intrinsic biliary clearance (calculated based on intracellular concentrations instead of medium concentrations) is more reflective of in vivo biliary clearance.[45] In addition, quantitative proteomic approaches have been applied to improve biliary clearance predictions, as discussed in detail in the “Mechanistic and PBPK Modeling” section.

Basolateral efflux clearance can be estimated by preloading SCH with a substrate, and measuring the medium concentration at the end of the efflux phase. Ferslew et al. estimated basolateral efflux clearance of enalaprilat (generated in hepatocytes after incubation of rat SCH with enalapril) based on the cumulative amount of enalaprilat effluxed into the medium and intracellular enalaprilat concentrations over the efflux period.[46] The functional importance of MRP4 in the basolateral efflux of enalaprilat was demonstrated by using MK-571, an inhibitor of multiple MRPs, in rat SCH, and confirmed in membrane vesicles prepared from HEK-293 cells overexpressing human MRP4. Of note, direct estimation of basolateral efflux using this approach was possible because biliary excretion of enalaprilat is negligible. For compounds that undergo extensive biliary excretion, mechanistic modeling is necessary to deconvolute basolateral efflux, biliary excretion, and flux from the bile compartment to the medium, as discussed in the “Mechanistic and PBPK Modeling” section.

Transporter-Mediated DDIs—Transporter-based drug-drug and drug-bile acid interactions may have significant toxicological implications, such as statin-induced myopathy and rhabdomyolysis due to inhibition of OATPs,[47] and troglitazone (TGZ)- and bosentan-induced hepatotoxicity due to inhibition of BSEP.[48,49] Membrane vesicles prepared from transfected cells overexpressing relevant transport proteins are useful to characterize substrate specificity and inhibitory potency of a given transport protein in isolation. However, a more physiologically representative, organ-specific, whole-cell system is needed to elucidate the relative contribution of individual transporters to overall clearance, and to estimate the net effect of inhibition/induction at multiple sites. Both acute (direct and indirect) and long-term effects on transporters have been studied in SCH.

A DDI between ritonavir (perpetrator) and ^{99m}Tc–mebrofenin (victim substrate) due to direct inhibition was demonstrated by Pfeifer et al. using human SCH coupled with modeling and simulation of clinical data.[6,50] Ritonavir decreased ^{99m}Tc–mebrofenin uptake without changing the BEI of ^{99m}Tc–mebrofenin, despite the fact that ritonavir had been reported to inhibit MRP2, which mediates the biliary excretion of ^{99m}Tc–mebrofenin. These in vitro findings were consistent with the clinical observation that single or multiple doses of ritonavir increased ^{99m}Tc–mebrofenin systemic exposure without significantly changing biliary recovery of ^{99m}Tc–mebrofenin. SCH data revealed that intracellular ritonavir concentrations after clinical doses were not high enough to inhibit MRP2 based on data generated for ^{99m}Tc–mebrofenin transport by MRP2.

Unlike direct inhibition, indirect inhibition of transporters is under-appreciated and the relevant studies using SCH are still limited. Powell et al [51] reported post-translational regulation of OATP1B3 by the protein kinase C (PKC) activator, phorbol-12-myristate-13-acetate (PMA). This mechanism was revealed by the fact that pre-treatment of SCH with PMA inhibited OATP1B3 function while co-incubation with PMA did not. Kruglov et al. reported that the type II inositol 1,4,5-trisphosphate receptor modulates Bsep activity in rat SCH through post-translational regulation.[52] The important role of N-glycosylation of ATP-binding cassette transporters on transport activity was established using rat SCH.[53,54]

The induction of transporters after long-term incubation (>24 hr) also was studied in SCH. Up-regulation of transporter mRNA expression in response to prototypical activators of the

pregnane X receptor, aryl hydrocarbon receptor and constitutive androstane receptor were reported in mouse SCH.[55] In addition to changes in mRNA expression of P-gp, an increase in the BEI of digoxin, a P-gp substrate, was observed in human SCH following treatment with rifampicin for 3 days.[56]

Enzyme-Transporter Interplay

The complexity of DDI predictions may be increased further by the interplay between enzymes and transporters. Many compounds interact with enzymes and transporters simultaneously. For example, cyclosporine inhibits CYP3A4, and multiple transporters including P-gp and OATP1B1. Gemfibrozil and gemfibrozil glucuronide inhibit CYP2C8 and OATP1B1.[47] Moreover, the parent compound and derived metabolites may have similar or opposite effects on transporters and enzymes. For drugs that are metabolized extensively, the presence of metabolic capacity in SCH enables the simultaneous evaluation of parent and metabolite effects without prior knowledge regarding the metabolites. This capability is very beneficial, especially in the early stages of drug discovery when metabolite identification has not been conducted and purified metabolites are not available. A few examples are discussed below.

For drugs that are rapidly metabolized and the metabolites are not transporter inhibitors, the intracellular concentration of the parent compound might not be high enough to inhibit efflux transporters. For example, cilexetil (CIL) exhibited potent BSEP inhibition based on membrane vesicle assays. However, BSEP inhibition by CIL was not observed in human SCH after 120-min exposure, which might be due to the metabolic elimination of CIL in SCH.[57] In this case, the membrane vesicle data led to a false positive prediction of BSEP inhibition. Sometimes metabolites are more potent inhibitors of transporters, such as TGZ sulfate vs. TGZ. In this case, data from a metabolism-deficient system could lead to false-negative results.[49] The interplay between formation and excretion of TGZ metabolites was studied in rat SCH lacking Bcrp and Mrp2 by Yang et al. using RNA interference techniques to knock down Bcrp in SCH prepared from TR^- rats.[58] In some cases, only the metabolites are transporter inhibitors. For example, although estradiol and bilirubin do not inhibit MRP2, pre-exposure of rat SCH to estradiol and bilirubin decreased the biliary excretion of 5-(and 6)-carboxy-2′,7′-dichlorofluorescein, a MRP2 substrate, which could be attributed to the inhibition by the generated metabolites of estradiol and bilirubin.[59]

Mechanistic and PBPK Modeling

Physiologically based pharmacokinetic (PBPK) modeling is a useful tool to predict the pharmacokinetics of novel compounds in the systemic circulation and target organs. Successful PBPK models depend on reliable estimates of compound-specific information (e.g., clearance, tissue partition coefficients, and the rate and extent of absorption). SCH have been used to estimate clearance values that are incorporated into PBPK models. The methods to estimate in vitro clearance using SCH and extrapolate from in vitro to in vivo clearance values are discussed below.

In vitro intrinsic uptake and efflux clearance values have been estimated using empirical methods, as described in the previous sections. The apparent clearance value determined

from SCH data may be comprised of more than one clearance pathway. Despite this limitation, clearance values estimated by empirical/static approaches can represent useful prior information to guide the experimental design for mechanistic modeling and simulation, and generally requires a relatively small number of data points.

Mechanistic pharmacokinetic models have been developed to deconvolute apparent uptake and efflux clearance values and obtain more accurate estimates. Linear kinetics are assumed and the clearance terms (rather than V_{max} and K_m) are used because a single, low concentration of substrate typically is studied. To estimate the kinetic parameters, multiple time points during both the uptake and efflux phase are required. Depending on the permeability of the substrate, passive diffusion clearance could be estimated solely from 37°C data. The kinetic parameters estimated could be used to perform sensitivity analyses and Monte Carlo simulations, which can help identify key model input parameters. Depending on the model structure and complexity, the published mechanistic pharmacokinetic models are classified into three categories. The model structures and exemplar experimental protocols are shown in Figure 2; the model output parameters, assumptions and applications of each model are summarized in Table 1.

Model I—This model is the simplest for the SCH system (Figure 2A). Three compartments represent the medium, cell, and bile, with passive diffusion, active uptake, biliary efflux, and metabolism processes included. Key kinetic parameters include intrinsic passive diffusion clearance ($CL_{int,\ pass}$); intrinsic uptake clearance ($CL_{int,\ uptake}$), and intrinsic biliary clearance ($CL_{int,\ bile}$). Basolateral efflux is assumed to be negligible. When significant metabolism is observed, intrinsic metabolic clearance ($CL_{int,\ met}$) is set to the unbound intrinsic clearance value determined in HLMs. To generate the experimental data, SCH are first pre-incubated with standard HBSS, Ca^{2+}-free HBSS, or standard HBSS containing rifamycin SV, followed by incubation with the substrate. Substrate uptake is terminated at different time points, and the intracellular and medium concentrations of the substrate are measured. This model has been applied to estimate the in vitro intrinsic clearance for OATP substrates by several research groups.[60_62]

Model II—Unlike Model I where $CL_{int,\ met}$ is fixed to a pre-determined value, $CL_{int,\ met}$ is fitted to metabolite(s) concentration- time data in Model II. In addition, intrinsic basolateral efflux clearance of metabolite ($CL_{int,\ BL,\ metabolite}$) is included rather than assuming passive diffusion. $K_{flux,\ metabolite}$, which accounts for the "flux" of metabolite from the canalicular compartment into the buffer, also is incorporated.[68_70] In this model, it is assumed that only metabolites undergo efflux into bile or medium. (Figure 2B). The experimental protocol is similar to that of Model I except that the pre-incubation phase only consists of two conditions (HBSS and Ca^{2+}-free HBSS) and both parent and metabolite(s) concentrations are measured. Lee et al. fitted this model to concentration-time data for TGZ and metabolites [TGZ sulfate, TGZ glucuronide, and TGZ quinone] in rat and human SCH.[63] This model has been used to characterize the contribution of individual clearance pathways to the disposition of mycophenolic acid (MPA) and MPA glucuronide (MPAG),[64] and the inhibitory potency of cyclosporine on each pathway in human SCH.[67] The modeling results suggest that cyclosporine A inhibits both basolateral uptake and biliary efflux clearance of

MPAG without changing the conversion of MPA to MPAG. This mechanism explains the cyclosporine A-mediated decrease in enterohepatic circulation of MPAG and lower systemic exposure of MPA and MPAG in humans.

Model III—Model III is more suitable for compounds with minimal passive diffusion that are not extensively metabolized (Figure 2C), such as rosuvastatin (RSV) and TCA. To obtain an accurate estimate of basolateral efflux, a novel uptake and efflux protocol is used, which includes an uptake phase followed by an efflux phase where serial samples are obtained. Uptake, biliary, and basolateral efflux clearance values for RSV, ^{3}H-TCA, and d_8-TCA were estimated from rat and human SCH data.[65–67] The impact of impaired clearance of RSV and ^{3}H-TCA were simulated, and predicted perpetrator effects on $d_{8\text{-TCA}}$ disposition were compared with experimental observations.

In this experimental design, a few practical factors need to be considered for determining the maximum incubation time. Most of the time, the uptake phase is extended beyond the linear range to attain steady-state intracellular conditions, which reduces the error in certain parameter estimates observed with shorter incubation times.[71] However, exposure to Ca^{2+}-free HBSS for more than 30 min increases cytotoxicity.[1] Therefore, after pre-incubation with Ca^{2+}-containing or Ca^{2+}-free HBSS for 10 min, SCH are incubated with Ca^{2+}-containing HBSS during the uptake phase. The uptake phase should be limited to 20 min in Ca^{2+}-containing HBSS to avoid resealing of tight junctions in SCH pre-incubated with Ca^{2+}-free HBSS.[65]

Scaling Methods—In vivo intrinsic clearance is a key parameter for PBPK models that can be extrapolated from in vitro clearance using the following scaling methods. The simplest and most straightforward approach of scaling up is based on hepatocellularity and liver weight as described previously[72] and reviewed by Poulin.[73] Scaling with physiological parameters works well for metabolic clearance. However, this approach leads to an underprediction of $CL_{int,\ uptake}$ and an overprediction of $CL_{int,\ bile}$.[60] Underprediction of uptake may be due to disregarding $CL_{int,\ BL}$ in the model, or to down-regulation of uptake transporters in vitro compared to in vivo[14]. Overprediction of $CL_{int,\ bile}$ may be due the absence of enterohepatic recirculation, and/or ignoring $_{Kflux}$ in the mechanistic model.[60] Clearly, over-simplification of the model structure can lead to over- or under-prediction of parameters. To address this issue, Jones et al. determined compound-specific empirical scaling factors (SFs) by comparing in vivo clearance estimated from intravenous pharmacokinetic data to in vitro clearance data;[60] geometric mean SFs for intrinsic unbound uptake clearance ($CL_{int,\ u,\ uptake}$), intrinsic unbound biliary clearance ($CL_{int,\ u,\ bile}$) and intrinsic unbound passive diffusion clearance ($CL_{int,\ u,\ pass}$) of seven OATP substrates were reported as 58, 0.061, and 1.[60] These SFs have been used in the in vitro-in vivo extrapolation of other OATP substrates such as telmisartan.[60,61] A similar approach has been applied to estimate SFs for $CL_{int,\ uptake}$ of pravastatin, repaglinide, and glyburide.[74–76] Li et al. developed a single set of empirical SFs by simultaneously modeling data for the same seven OATP substrates; they reported SFs of 55 for $CL_{int,\ u,\ uptake}$, 0.019 for $CL_{int,\ u,\ bile}$, and 0.092 for $CL_{int,\ u,\ pass}$.[77] The difference in the estimated SF for $CL_{int,\ u,\ pass}$ between the two studies (1 vs. 0.092) could be due to different approaches for model fitting [the SF for

intrinsic unbound metabolic clearance ($CL_{int, u, met}$) was not estimated by Jones et al.[60] because $CL_{int, u, met}$ was not identifiable, but this SF was fitted in the work of Li et al.[77]]

The approach described above relies on intravenous pharmacokinetic data to estimate empirical SFs. If intravenous data are not available, the in vitro-in vivo extrapolation could be facilitated by information regarding transporter abundance. Absolute quantification of transporter expression by mass spectrometry was first reported by Terasaki and colleagues, based on the assumption that all expressed protein is localized on the membrane and, therefore, functional.[78–82] This technique has been advanced by the work of Lai and coworkers,[10, 13, 24, 83] Unadkat and colleagues [78, 79] and more recently by Artursson and coworkers [84] and Galetin and colleagues.[85]

Intrinsic clearance values estimated using the approaches detailed above can be used directly in PBPK models [86] or they can be combined with liver blood flow and protein binding data to estimate hepatic clearance based on the well-stirred or parallel-tube models of hepatic disposition.[87] Pharmacokinetic profiles have been predicted successfully for numerous compounds including statins, sartans, mebrofenin, pafuramidine, glyburide, and repaglinide using PBPK models that incorporated clearance values estimated from SCH.[24, 50, 60–62, 74–76, 88–91]

USE OF SANDWICH–CULTURED HEPATOCYTES TO STUDY DRUG–INDUCED LIVER INJURY

Drug-induced liver injury (DILI) is the most common cause of acute fulminant hepatic failure,[94] and is the primary reason for withdrawal of approved drugs from the market.[95] DILI is one of the major challenges during drug development because standard preclinical testing has not been able to precisely predict clinical DILI and mechanisms underlying interspecies differences have not been fully elucidated. DILI manifests as a broad spectrum of liver injuries, and multiple mechanisms may cause DILI including oxidative stress, mitochondrial toxicity, and bile acid transporter inhibition.[96, 97] Therefore, many different approaches and experimental systems have been used to predict the hepatotoxic potential of compounds. SCH are a useful tool to assess cytotoxicity and perturbation of biological processes by drugs and hepatically-generated metabolites, providing mechanistic insights into hepatotoxicity.[98–100] This system also allows direct sampling of hepatocytes for measurement of intracellular drug exposure or cytotoxicity endpoints such as ATP.

In this section, use of SCH to study DILI is reviewed with a focus on bile acid-mediated hepatotoxicity. Mechanistic investigations of altered bile acid disposition by drugs using SCH and mechanistic modeling are reviewed first. Next, use of systems pharmacology modeling to predict clinical DILI is discussed. An example of how the SCH model was used to establish a quantitative relationship between intracellular bile acids and toxicity in a systems pharmacology model is presented using novel unpublished data generated in our laboratory.

Mechanistic Investigations of Bile Acid-Mediated DILI

One proposed mechanism of DILI is inhibition of bile acid efflux in hepatocytes by drugs, which may result in intracellular accumulation of potentially toxic bile acids.[101,102] Evidence continues to accumulate that inhibition of bile acid transporters such as BSEP and MRPs by drugs is a risk factor for DILI.[103–106] Bile acids play important roles in the body as key signaling molecules as well as lipid solubilizers, but bile acids can be cytotoxic when present at supraphysiologic concentrations in hepatocytes.[107] Bile acid toxicity is highly correlated with hydrophobicity; lithocholic acid (LCA), chenodeoxycholic acid (CDCA), and deoxycholic acid (DCA) are more cytotoxic than less hydrophobic bile acids, cholic acid (CA) and ursodeoxycholic acid (UDCA).[101,108,109] Mechanisms of bile acid-induced hepatotoxicity include disruption of cell membranes due to their detergent-like properties, disruption of mitochondrial ATP synthesis, necrosis, and apoptosis.[101]

Hepatic enzymes and transport proteins play important roles in metabolism and excretion of bile acids.[110–113] SCH express bile acid metabolizing enzymes and transporters, and are capable of synthesizing, metabolizing, and transporting bile acids.[114] SCH also can be isolated from different species, enabling investigation of species differences in hepatobiliary bile acid disposition and drug-bile acid interactions, as reviewed in the following section.

Characterization of Hepatobiliary Bile Acid Disposition in SCH—Vectorial transport of bile acids is mediated primarily by the hepatic uptake transporter NTCP and the canalicular efflux transporter BSEP.[111,112] In addition to BSEP-mediated biliary excretion, bile acids also can be transported into sinusoidal blood by MRP3, MRP4, and organic solute transporter (OST)α/β.[115–118] Due to extensive biliary excretion, the contribution of basolateral efflux to hepatocellular bile acid excretion was presumed to be minimal. However, mechanistic modeling based on TCA disposition data in rat SCH demonstrated that $CL_{int,\ bile}$ and $CL_{int,\ BL}$ of TCA are similar (0.34 and 0.26 mL/min/gram liver, respectively).[119] These data suggest that biliary excretion and basolateral efflux contribute almost equally to hepatocellular excretion of TCA in rat SCH. Bile acids transported into sinusoidal blood can subsequently be taken up by downstream hepatocytes. After undergoing blood-liver cycling as they move from the periportal to the centrilobular zone, the majority of bile acids eventually are excreted into bile, similar to the “hepatocyte hopping” of bilirubin glucuronides.[120] In contrast, biliary excretion of TCA predominated in human SCH ($CL_{int,\ bile}$=0.14 mL/min/gram liver and $CL_{int,\ BL}$=0.042 mL/min/gram liver), indicating that species differences exist in the hepatocellular excretion of bile acids in rats vs. humans.[119]

SCH also can be used to investigate bile acid disposition in hepatocytes from special populations such as the fetus. Sharma et al. showed that the BEI of TCA, a BSEP substrate, in fetal hepatocytes was approximately one-half of that in adult hepatocytes (36 and 72%, respectively).[121] RT-PCR analysis demonstrated that mRNA expression of *ABCB11* (a gene encoding BSEP) in fetal hepatocytes was 40% of that in adult hepatocytes, consistent with the functional study results.[121]

Evaluation of Drug Effects on Hepatobiliary Bile Acid Disposition using SCH—Drug effects on bile acid transport can be evaluated using multiple in vitro systems. Isolated membrane vesicles overexpressing a specific transporter (e.g., BSEP, MRP3, MRP4) have been used widely to assess drug-bile acid interactions that involve efflux transporters.[103,104,106,122] To assess drug effects on hepatic uptake of bile acids, cell lines overexpressing uptake transporters (e.g., NTCP) are employed. These transporter-overexpressing systems provide a useful tool to study drug-bile acid interactions for a single transporter, and to estimate kinetic parameters of bile acid transport and drug-mediated inhibition [e.g., Michaelis-Menten constant (K_m), inhibition constant (K_i), half-maximal inhibitory concentration (IC_{50})]. However, it is difficult to assess the "net effect" of drugs on hepatobiliary bile acid disposition using these systems because multiple uptake and efflux transporters are involved in bile acid disposition. SCH, which express functional bile acid transporters on the basolateral and canalicular membranes, are suitable for this purpose. SCH also express functional metabolic enzymes and allow evaluation of drug metabolite effects on bile acid transporters, which is advantageous when the metabolic pathways have not been characterized and/or the specific effects of metabolites are unknown.

SCH have been used widely to determine altered bile acid disposition by drugs that belong to different therapeutic classes. Endothelin receptor antagonists (ERAs) are used to manage pulmonary arterial hypertension. Despite their clinical benefits, some ERAs have been associated with hepatotoxicity, although the incidence rate and severity appears to be compound-specific. Sitaxsentan was withdrawn from the market recently due to cases of fatal hepatotoxicity, and bosentan requires monthly monitoring due to serum aminotransferase elevations in a subset of patients.[123–125] Inhibition of bile acid transporters has been proposed as an underlying mechanism of sitaxsentan- and bosentan-mediated DILI.[103,126,127] On the other hand, recently approved ERAs, ambrisentan and macitentan, are associated with a lower risk of liver injury.[128–130] Studies using human SCH demonstrated that individual ERAs have differential effects on the hepatobiliary disposition of bile acids. In human SCH, bosentan and macitentan significantly decreased the BEI and apparent biliary clearance of TCA, whereas ambrisentan showed minimal inhibitory effects on TCA biliary excretion.[30] Bosentan and sitaxsentan also significantly inhibited sodium-dependent TCA uptake in human SCH.[30] As a result of inhibitory effects on multiple bile acid transporters, bosentan and macitentan significantly decreased total (cell + bile) and cellular accumulation of TCA in human SCH in a concentration-dependent manner.[30] Interestingly, individual ERAs accumulated in human SCH to a different extent; the hepatocyte concentration of macitentan was about 100-fold greater than the medium concentration followed by sitaxsentan (40-fold), bosentan (20-fold), and ambrisentan (2-fold).[26] The low incidence of macitentan hepatotoxicity in the clinic may be due to the low dose and relatively lower exposure compared to the other ERAs. Hepatocyte concentrations of these inhibitors at clinically relevant doses need to be investigated to confirm this hypothesis.

Antiretroviral protease inhibitors (PIs) are commonly used to treat human immunodeficiency virus, but in a subset of patients, their clinical use is limited due to DILI.[132–134] Ritonavir is often administered with other PIs to improve oral bioavailability of the coadministered PIs,

but ritonavir-containing regimens are associated with an 8.6-fold increase in the risk of hepatotoxicity.[133] Several PIs including ritonavir and lopinavir are known to inhibit BSEP,[103,135] suggesting that hepatotoxicity is mediated, in part, by bile acid transport inhibition. Studies in rat SCH demonstrated that ritonavir and lopinavir significantly reduced TCA biliary excretion (BEI and $CL_{b, app, in vitro}$) and subsequently, increased intracellular accumulation of TCA.[136] Co-incubation of both lopinavir and ritonavir further decreased biliary excretion, resulting in increased cellular TCA accumulation.[136] Interestingly, 24-hr exposure to lopinavir and ritonavir decreased hepatic accumulation of endogenous bile acids in rat SCH, potentially due to protective feedback regulation that reduced hepatic bile acid synthesis.[136]

TAK-875 is a selective G-protein-coupled receptor 40 agonist that was developed to treat type 2 diabetes, but the clinical development of TAK-875 was discontinued due to hepatotoxicity concerns. Studies using rat SCH demonstrated that TAK-875 decreased $CL_{b, app, in vitro}$ and BEI of TCA, suggesting that inhibition of bile acid transport may be responsible, in part, for the hepatotoxicity of this compound.[137]

Guo et al. reported that alpha-naphthylisothiocyanate (ANIT), a model cholestatic compound, induced total bile acid accumulation in rat SCH after a 48-hr incubation, which was consistent with elevated total serum bile acids after in vivo exposure in rats. This effect of ANIT was probably due to inhibition of Ntcp, Oatp1a4 and/or Oatp1a1, Mrp2, and Mrp3, as demonstrated by using prototypical transporter substrates, but not because of increased bile acid synthesis, as evidenced by decreased mRNA expression of enzymes governing bile acid synthesis (i.e., Cyp7a1, Cyp27a1, and Cyp8b1).[138]

Investigation of a panel of endpoints in SCH (e.g., BEI, $CL_{b, app, in vitro}$, total and cellular accumulation of bile acids) provides mechanistic information about potential sites (uptake or excretion) of bile acid transporter modulation by compounds. For example, if a compound inhibits both uptake (indicated by a decrease in total accumulation and $CL_{b, app, in vitro}$) and biliary excretion (indicated by a decrease in BEI and $CL_{b, app, in vitro}$) of bile acids, an increase in cellular accumulation of bile acids suggests that the compound predominantly influences biliary excretion. On the other hand, a decrease in the cellular accumulation of bile acids indicates that bile acid uptake is primarily affected. Ansede et al. investigated the effects of TGZ, glyburide, cyclosporine A, and erythromycin estolate on the disposition of the model bile acid TCA in rat SCH. These compounds had been shown to inhibit hepatic bile acid transporters in isolated vesicular systems or suspended hepatocytes.[103,104,139,140] Based on SCH data using endpoint analysis, as described above, cyclosporine A and glyburide inhibited biliary excretion to a greater extent than hepatic uptake of TCA. On the other hand, erythromycin estolate and TGZ primarily affected TCA uptake.[140,141] These examples demonstrate that unlike other in vitro transporter models, SCH can be used to simultaneously determine the effects of a drug on the basolateral uptake and biliary excretion of bile acids, and therefore, the overall effect of drugs on the hepatobiliary disposition of bile acids can be assessed. In addition, for drugs like TGZ, where the metabolite (e.g. TGZ sulfate) is a more potent inhibitor of transporters compared to the parent,[142] SCH data reflect the combined effects of both the parent and the metabolite, providing more physiologically-relevant information.

Pedersen et al. compared the inhibition of TCA canalicular efflux by drugs associated with severe DILI and less severe/no DILI in human SCH.[106] They reported that drugs associated with severe DILI such as cyclosporine A, ritonavir, rosiglitazone, and TGZ significantly reduced the canalicular efflux of TCA. On the other hand, drugs with less severe or no DILI (i.e., mifepristone, isradipine, budesonide, and glyburide) showed minimal effects on the canalicular efflux of TCA in human SCH, despite the fact that they exhibited similar potency towards BSEP inhibition in membrane vesicle assays. These results suggest that human SCH can decrease false positives that occur with membrane vesicle assays and thus, can be used to differentiate BSEP inhibitors associated with severe DILI from those with less DILI liabilities. A study by Chatterjee et al. also concluded that SCH are a useful model system to predict hepatotoxic potential of drugs mediated by bile acid transport inhibition.[143] In their study, a urea assay was performed after incubation of human SCH with cholestatic and non-cholestatic compounds to assess functional changes in hepatocytes. The drug-induced cholestatic index (DICI), the relative residual urea formation in SCH co-incubated with drugs and bile acids as compared to urea formation in SCH incubated with drugs alone, was calculated. Cholestatic compounds (e.g., cyclosporine A, TGZ, chlorpromazine, bosentan, ticlopidine, ritonavir, and midecamycin) showed DICI≤0.8, indicating that these compounds had enhanced toxicity (reduced urea formation) in the presence of bile acids. Conversely, non-cholestatic compounds (e.g., diclofenac, valproic acid, amiodarone, and acetaminophen) showed DICI > 0.8 because cytotoxicity of compounds remained unchanged with bile acid co-incubation. Overall, these studies confirm the utility of SCH for early screening of DILI mediated by bile acid transport inhibition.

Use of Human-Relevant Bile Acids to Characterize Drug–Bile Acid Interactions in SCH—TCA, which has been used widely as a model bile acid to investigate drug-bile acid interactions, is a predominant bile acid species in rodents, whereas its contribution to the human bile acid pool is minor.[144] On the other hand, CDCA and its conjugates are prevalent primary bile acids in humans.[144] TCA, a conjugated trihydroxy bile acid, is less hydrophobic, and thus, less toxic, compared to the dihydroxy bile acid CDCA.[101] Interestingly, Marion et al. reported that TGZ had differential effects on hepatobiliary disposition of TCA and CDCA.[139] TGZ decreased cellular accumulation of TCA in rat SCH, consistent with earlier reports as described in the “Evaluation of Drug Effects on Hepatobiliary Bile Acid Disposition using SCH” section, but increased CDCA accumulation in hepatocytes.[139] Subsequent studies revealed that TGZ significantly inhibited TCA uptake in suspended rat hepatocytes, whereas uptake of CDCA, which was mediated by a nonsaturable sodium-independent mechanism, was less affected by TGZ. Griffin et al. also reported that while lopinavir and ritonavir significantly decreased biliary excretion of both TCA and CDCA, only TCA showed increased cellular accumulation; intracellular CDCA levels remained unchanged.[136] These data suggest that drugs have differential effects on individual bile acids, and that altered TCA disposition may not be representative of the disposition of other bile acids. Therefore, use of human-relevant, more cytotoxic bile acids (e.g., CDCA) may provide better insights into human DILI.

Use of Fluorescent Bile Acids as Probes to Characterize Drug–Bile Acid Interactions in SCH—Fluorescent bile acids are another useful tool to assess drug effects

on hepatobiliary disposition of bile acids. One advantage of fluorescent bile acids is that they can be visualized by microscopic and confocal imaging, allowing non-invasive assessment of hepatic bile acid disposition and high-throughput screening. Aminofluorescein-tagged bile acids, chenodeoxycholylglycylamidofluorescein (CDCGamF) and cholylglycylamidofluorescein (CGamF), have been employed to assess drug effects on bile acid transport in transfected cells and membrane vesicle systems.[145] Interestingly, species differences were observed in the effects of PIs on CGamF disposition in SCH; atazanavir, indivanir, and darunavir potently inhibited CGamF accumulation in human SCH, whereas inhibitory effects in rat, dog, and pig SCH were less significant.[146] Cholyl-L-lysyl-fluorescein (CLF) is another fluorescent bile acid analogue that has been used to study drug-bile acid interactions. Barber et al. quantified inhibition of CLF disposition by twenty-nine drugs in rat SCH.[147] They estimated IC_{50} values for biliary excretion of CLF, and reported that all of the drugs that showed plasma C_{max}/IC_{50} ratios > 0.1 were associated with DILI in humans. Interestingly, for many compounds tested, IC_{50} values on CLF biliary excretion measured in rat SCH were smaller than IC_{50} values measured in membrane vesicle systems from cells expressing BSEP or MRP2, suggesting the potential contribution of metabolites formed in SCH. Of note, unlike endogenous bile acids, hepatic uptake of CGamF and CLF is mediated predominantly by OATP, and MRP2 rather than BSEP is primarily responsible for the biliary excretion of CLF.[146,148] A recently developed fluorescent bile acid derivative, N-(24-[7-(4-N,N-dimethylaminosulfonyl-2,1,3-benzoxadiazole)]amino-3α,7 α,12 α-trihydroxy-27-nor-5β-cholestan-26-oyl)-2′-aminoethanesulfonate (tauro-nor-THCA-24-DBD), was shown to be transported by NTCP and BSEP in human and rat SCH, similar to endogenous bile acids; this may prove to be a useful probe for drug-bile acid interaction studies.[149] Overall, fluorescent bile acids in the SCH system are a useful tool to study drug and metabolite effects on bile acid disposition in a physiologically relevant system by live cell analysis of bile acid biliary excretion.

Integration of SCH Data into a Systems Pharmacology Model to Predict DILI

As reviewed in the previous section, SCH data provide useful insights in terms of drug-bile acid interactions. These in vitro data can be integrated with physiological knowledge using a systems pharmacology modeling approach to predict clinical hepatotoxicity. Systems pharmacology modeling is a useful tool to translate mechanistic data measured in vitro to in vivo. DILIsym® is a quantitative systems pharmacology model of DILI that includes drug disposition and physiological processes involved in DILI. Multiple mechanisms of DILI including oxidative stress, mitochondrial dysfunction, and bile acid transport inhibition are represented within DILIsym®, enabling prediction of DILI in humans and preclinical animals.[150–152] To predict bile acid-mediated DILI, a bile acid homeostasis sub-model was constructed within DILIsym®.[153] However, to construct the sub-model, the intracellular bile acid concentrations that led to hepatotoxicity needed to be quantified. The relative potency of bile acids with respect to hepatotoxicity was investigated based on medium concentrations or systemic exposure using in vitro and in vivo systems,[154,155] but the relationship between hepatocellular bile acid concentrations and toxicity had not been determined quantitatively. In this section, a case study is presented to demonstrate how SCH data were used to fill this data gap, which is essential to link bile acid kinetics to toxicity in a bile acid transport inhibition sub-model within DILIsym®.

Bile Acid Toxicity Studies in SCH to Establish a Quantitative Relationship Between Hepatocellular Bile Acids and Toxicity—The current study investigated cellular exposure and toxicity of LCA and CDCA in human and rat SCH. LCA and CDCA were chosen because they are hydrophobic and potentially toxic bile acid species; LCA is a secondary bile acid formed by bacterial metabolism of CDCA in the intestinal lumen.[101] Hepatic metabolic pathways and hydrophobicity of CDCA and LCA are summarized in Figure 3.

On day 3 (rat) or 6 (human) of culture, SCH were incubated with LCA (0.025, 0.05, 0.1, 0.125, 0.15, and 0.2 mM), CDCA (0.05, 0.1, 0.25, 0.375, 0.5, and 1 mM for rat SCH; 0.25, 0.375, 0.5, 0.65, 0.8, and 1 mM for human SCH), 0.1 % DMSO (vehicle control), or 2 % Triton-X (positive control) for 6, 12, and 24 hr. After bile acid incubation, cytotoxicity (cellular ATP concentrations and LDH leakage) and intracellular bile acid concentrations were measured. Cytotoxicity was assessed by LDH release from damaged cells using the LDH-Cytotoxicity Detection Kit according to the manufacturer's protocol. Data were corrected for baseline levels in vehicle control (0.1% DMSO-treated SCH) and presented as a percentage of positive control (2% Triton X-100-treated SCH) using the following equation;

$$\text{Cytotoxicity}\ (\%)=\frac{\text{absorbance of samples}-\text{absorbance of vehicle control}}{\text{absorbance of positive control}-\text{absorbance of vehicle control}}\times 100 \quad \text{Eq. 4}$$

The values measured after complete cell lysis using 2% Triton X-100 were considered as maximum cell death (100% cytotoxicity). Intracellular ATP levels were measured using CellTiter-Glo® Luminescent Cell Viability Assay Kit according to the manufacturer's protocol. Intracellular ATP concentrations were calculated by dividing ATP amount (pmol/well) by cellular volume (1.26 μl/well),[156] and values were corrected for cell viability obtained from the LDH assay using the following equations;

$$\text{Cellular ATP concentration of viable cells}\ (\text{mM})=\frac{\text{ATP amount}}{\text{Cellular volume}}\times\frac{1}{\text{Fraction viable cells}} \quad \text{Eq. 5}$$

$$\text{Fraction viable cells}=\frac{100-\%\,\text{cytotoxicity}}{100} \quad \text{Eq. 6}$$

For quantification of intracellular bile acids, hepatocytes were incubated with Ca^{2+}-free HBSS for 5 min to open tight junctions using B-CLEAR® technology (Qualyst Transporter Solutions, LLC, Durham, NC). Cell lysate samples were prepared and analyzed using liquid chromatography coupled with tandem mass spectrometry (LC-MS/MS) analysis as described previously.[114] Intracellular bile acid concentrations were calculated by dividing the amount of bile acids (pmol/well) by the cellular volume (1.26 μl/well),[156] and corrected for cell viability obtained from the LDH assay, as described above for intracellular ATP calculations. The medium or total intracellular bile acid concentrations at the half-maximal toxicity were estimated by performing non-linear regression analysis using a four parameter logistic model (GraphPad Prism version 6, La Jolla, CA).

Toxicity and Intracellular Bile Acid Exposure in LCA-Treated Rat and Human SCH—LCA, which is formed by bacterial 7α-dehydroxylation of CDCA in the gut lumen, has been reported to be the most hydrophobic and toxic bile acid species. Animals administered LCA have been used as a model of intrahepatic cholestasis.[157,158] In the present study, LCA showed differential toxicity in SCH from rats and humans. In rat SCH, treatment with 0 – 0.2 mM LCA exerted a concentration-dependent decrease in cellular ATP and increase in LDH leakage (Figure 4A). In human SCH, LCA caused a delayed decrease in cellular ATP and minimal LDH leakage was observed (Figure 4A).

To establish a quantitative relationship between LCA-induced toxicity and hepatocellular exposure to LCA species, cellular concentrations of LCA and LCA conjugates were measured in LCA-treated SCH by LC/MS/MS analysis. In rat SCH, unconjugated LCA accumulated extensively (in low mM ranges) and correlated with the observed toxicity (Figure 4B). Interestingly, TLCA and GLCA cellular concentrations were decreased at LCA medium concentrations greater than 0.1 mM (Figure 4B), potentially due to altered (e.g., saturation, depletion) glycine- or taurine-conjugation, adaptive increases in hepatic efflux of these conjugates, or further metabolism (e.g., sulfation). Intracellular concentrations of LCA and GLCA in human SCH were comparable to those in rat SCH, whereas TLCA concentrations in human SCH were ~100-fold lower than rat SCH (Figure 4B). Unlike rat SCH, intracellular TLCA and GLCA concentrations increased with increasing LCA medium concentrations up to 0.2 mM in human SCH (Figure 4B).

Concentrations at the half-maximal toxicity (LC_{50}) estimated based on medium or total intracellular LCA concentrations after 24 h incubation are presented in Table 2. In rat and human SCH, LC_{50} values based on total intracellular LCA concentrations were ~4–5-fold greater compared to those based on medium LCA concentrations due to extensive hepatic accumulation of unconjugated LCA (Table 2). These results suggest that estimation of LCA potency based on medium concentrations might overestimate the actual potency of LCA at the site of toxicity, if total intracellular concentrations are relevant to bile acid toxicity. On the other hand, LC_{50} values based on unbound intracellular LCA concentrations may be lower than those based on total intracellular LCA concentrations because of binding of bile acids to intracellular proteins or sequestration of bile acids within intracellular organelles. Assessment of unbound intracellular concentrations of bile acids by cell fractionation and binding studies will be necessary, if unbound concentrations are relevant to hepatotoxicity. It is also possible that bile acid concentrations within intracellular organelles that are sensitive

to bile acids (e.g., mitochondria) are more relevant to bile acid-mediated toxicity. To our knowledge, it still remains to be investigated whether bile acid toxicity is driven by total or unbound intracellular bile acid concentrations, or concentrations within sub-cellular organelles.

Toxicity and Intracellular Bile Acid Exposure in CDCA-Treated Rat and Human SCH—CDCA and conjugates are dominant bile acids in humans, whereas they contribute to a smaller proportion of the bile acid pool in rats and mice.[144,159–161] After incubation with 0 – 1 mM CDCA, medium concentration-dependent toxicity was observed in both rat and human SCH (Figure 5A). Human SCH showed delayed toxicity with a higher LC_{50} based on medium CDCA concentrations, suggesting that CDCA-mediated toxicity is less potent compared to rat SCH (Figure 5A, Table 2).

To establish a quantitative relationship between CDCA-induced toxicity and hepatocellular exposure to CDCA species, cellular concentrations of CDCA and its conjugates were measured in CDCA-treated SCH. In rat SCH, unconjugated CDCA and TCDCA increased with increasing CDCA medium concentrations, consistent with the observed toxicity (Figure 5B). Cellular TCDCA was ~100-fold lower compared to CDCA (Figure 5B); thus, it is plausible that unconjugated CDCA is associated with the observed toxicity in rat SCH. LC_{50} values estimated based on medium or total intracellular CDCA concentrations are presented in Table 2. Unlike LCA, LC_{50} values based on total intracellular CDCA concentrations were lower compared to those based on medium CDCA concentrations. This led to a lower intracellular LC_{50} of CDCA compared to LCA in rat SCH, suggesting that CDCA is a more potent toxicant than LCA. It is possible that other CDCA conjugates (e.g., sulfate, glucuronide) that were not measured in the current study might have contributed to the observed toxicity in SCH exposed to CDCA.

In human SCH, intracellular concentrations of all the measured CDCA species decreased at high CDCA medium concentrations where toxicity was observed (Figure 5B), so it is not clear which bile acid caused toxicity in human SCH. Further investigation of other CDCA metabolites may provide additional insight.

Incorporation of SCH Data into a Systems Pharmacology Model—To our knowledge, this is the first investigation that has established quantitative relationships between intracellular LCA and CDCA exposure and hepatocyte toxicity in multiple species. Species differences in intracellular concentrations and toxic effects of LCA and CDCA after exposure to the same medium concentrations of these bile acids were noted in the present studies. Using these *in vitro* data, species differences in bile acid toxicity were characterized, and quantitative relationships between intracellular concentrations of individual bile acids and toxicity were established. These relationships were incorporated into DILIsym® to link bile acid homeostasis and ATP dynamic sub-models.[162] The toxic effects of bile acids were linked to decreases in cellular ATP, which is an important determinant of cellular necrosis in DILIsym®. Subsequently, this model was successfully employed to predict clinical DILI mediated by drugs that interrupt bile acid transport such as TGZ and bosentan.[162,163] The relative safety of other BSEP inhibitors, pioglitazone and telmisartan, also was accurately predicted.[162,163] In addition, use of a species-specific bile acid homeostasis model[153] and

bile acid toxicity data obtained in the current study recapitulated species differences in hepatotoxicity of TGZ and bosentan.[162,163]

In the current study, intracellular LC_{50} levels were estimated in rat and human SCH based on the unconjugated LCA and CDCA concentrations because intracellular unconjugated LCA and CDCA concentrations were correlated with observed toxicity in rat SCH. However, it is possible that conjugated LCA and CDCA might cause toxicity.[164–169] Additional experiments (e.g., treatment of SCH with conjugates) would be needed to establish the relationship between intracellular concentrations of LCA and CDCA conjugates and toxicity. Also, in the present studies, *in vitro* toxicity was measured after short-term exposure to high concentrations of bile acids, assuming that toxicity was associated with direct effects on hepatocytes (e.g., mitochondrial proton gradient uncoupling). A different experimental approach would be necessary to examine the acute effects of bile acids on non-parenchymal cells, as well as the effects of long-term exposure to low concentrations of bile acids on both parenchymal and non-parenchymal cells.

Due to species differences in bile acid metabolism, substrate/inhibitor specificity of bile acid transporters, bile acid composition, and toxic effects of bile acids reported here and elsewhere, preclinical species do not reliably predict bile acid-mediated DILI in humans.[113,158,170,171] Mechanistic modeling incorporating data generated from human-derived *in vitro* systems such as human SCH would be expected to provide a more accurate approach to predict altered hepatic bile acid disposition and subsequent DILI in humans.

CONCLUSIONS AND FUTURE DIRECTIONS

SCH are a useful tool to study hepatobiliary drug disposition and underlying mechanisms of DILI. Hepatic drug metabolism and transport can be characterized in SCH from humans or from wild-type or transgenic animals, and combined with specific inhibitors, RNAi or other knockdown techniques. Application of new tools [e.g., Clustered Regularly Interspaced Short Palindromic Repeats (CRISPR)/CRISPR-associated 9 (Cas9) and targeted genome editing] to modulate gene expression in the SCH system may further improve characterization and prediction of hepatobiliary drug disposition. Kinetic parameters (e.g., metabolic and transporter-mediated clearances, inhibitory potency of compounds) can be estimated by mechanistic modeling of SCH data.[172] This information can be integrated into PBPK or systems pharmacology models to predict drug disposition, DDIs, or potential DILI in humans. Studies using SCH also can provide insight regarding mechanisms underlying drug-induced hepatotoxicity. Often, preclinical species are not predictive of bile-acid mediated DILI in humans. SCH have been used widely to investigate drug and/or metabolite effects on hepatobiliary disposition of bile acids, as discussed in the current manuscript. In addition, multiple mechanisms of hepatotoxicity can be screened simultaneously in the SCH system, when combined with recent technologies such as high content imaging.[173]

Isolation procedures, cryopreservation techniques, and culture conditions can significantly impact hepatocyte viability and expression/function of enzymes and transporters in SCH, which can influence data quality and variability. Therefore, use of carefully optimized, standardized protocols for preparing and culturing SCH is required to ensure reliable,

reproducible data. Use of commercially available, transporter certified hepatocytes or B-CLEAR® kits can minimize these issues. Appropriate quality controls (e.g., known probe substrates) for each experiment must be employed to ensure enzymes and/or transporters are functional. When isolated and cultured appropriately, variability in SCH data will reflect inherent variability in hepatocytes donors. Human SCH data would be expected to exhibit greater variability compared to SCH from preclinical species because of genetic polymorphisms, underlying diseases, medications, and environmental factors. Thus, depending on the purpose of the study, donor selection criteria need to be carefully pre-defined to minimize confounding effects. On the other hand, SCH isolated from special populations can be leveraged to study altered drug disposition in these populations (e.g., disease states, pediatrics, or geriatrics). Alternatively, culture conditions can be modified to induce disease-like characteristics (e.g., phospholipidosis, type II diabetes) or mimic specific physiological conditions (e.g., pregnancy) in SCH for the investigation of altered hepatobiliary disposition of drugs.[25,174,175]

Hepatocytes (parenchymal cells) account for about 60% of liver mass whereas non-parenchymal cells such as stellate cells, sinusoidal endothelial cells, and Kupffer cells constitute ~40% of the liver.[176] Although metabolic enzymes and transporters are expressed predominantly in hepatocytes, non-parenchymal cells also can influence drug disposition indirectly by modulating the function of enzymes and transporters through heterotypic cell-cell contacts and cytokine release. Cross-talk between hepatocytes and non-parenchymal cells can stimulate adaptive responses or aggravate toxic responses upon initiation of drug-induced hepatotoxicity. Therefore, co-culture of hepatocytes and non-parenchymal cells might better represent liver architecture and physiology. A recent study reported that co-culture of hepatocytes and liver sinusoidal endothelial cells in a sandwich configuration maintained their phenotypes and metabolic activity for up to four weeks.[177] Further investigations are needed to establish and characterize co-culture models of hepatocytes and various non-parenchymal cells.

The pioneering work of Dr. Ronald T. Borchardt and colleagues in establishing cell-based models (e.g., Caco-2 cells) to facilitate drug discovery and development inspired pharmaceutical scientists to develop new approaches to investigate drug disposition in vitro. One such system, the SCH model, is now a well-established tool to study hepatobiliary drug disposition, DDIs and DILI. In addition to serving as a useful screen in drug development, this model has improved mechanistic understanding of hepatocyte function. Further development, characterization, and meaningful refinements of the SCH model will advance our ability to effectively use this in vitro system to predict hepatic drug and metabolite disposition and toxicity. Importantly, evaluation of the factors that modulate hepatocyte function (e.g., disease states, medications, dietary constituents, and toxins), will lead to a greater understanding of hepatic transporters in health and disease.

Acknowledgments

This work was supported by the National Institute of General Medical Sciences of the National Institutes of Health (NIH) under Award Number R01 GM041935 (K.L.R.B) and by members of the DILI-sim Initiative. The content is solely the responsibility of the authors and does not necessarily represent the official views of the NIH. For more

information on the DILI-sim Initiative, see www.DILIsym.com. The authors thank Dr. Cassandra Hubert for her expert technical assistance in the analysis of bile acids.

Abbreviations used

ANIT	alpha-naphthylisothiocyanate
BEI	biliary excretion index
BSEP/Bsep	bile salt export pump
CA	cholic acid
CDCA	chenodeoxycholic acid
CDCGamF	chenodeoxycholylglycylamidofluorescein
CGamF	cholylglycylamidofluorescein
CIL	cilexetil
CLF	cholyl-L- lysyl-fluorescein
$\mathbf{CL_{b,\ app,\ in\ vitro}}$	in vitro apparent biliary clearance
$\mathbf{CL_{b,\ int,\ in\ vitro}}$	in vitro intrinsic biliary clearance
$\mathbf{CL_{int,\ uptake}}$	intrinsic uptake clearance
$\mathbf{CL_{int,\ pass}}$	intrinsic passive diffusion clearance
$\mathbf{CL_{int,\ bile}}$	intrinsic biliary clearance
$\mathbf{CL_{int,\ met}}$	intrinsic metabolic clearance
$\mathbf{CL_{int,\ BL}}$	intrinsic basolateral efflux clearance
$\mathbf{CL_{int,\ uptake,\ parent}}$	intrinsic uptake clearance of parent
$\mathbf{CL_{int,\ uptake,\ metabolite}}$	intrinsic uptake clearance of metabolite
$\mathbf{CL_{int,bile,\ metabolite}}$	intrinsic biliary clearance of metabolite
$\mathbf{CL_{int,\ BL,\ metabolite}}$	intrinsic basolateral efflux clearance of metabolite
$\mathbf{K_{flux,\ metabolite}}$	first-order rate constant for flux from bile networks into buffer of metabolite
Km	Michaelis-Menten constant
CYP	cytochrome P450
UGT	UDP-glucuronosyltransferase
SULT	sulfotransferase
DCA	deoxycholic acid

DDI	drug-drug interaction
DICI	drug-induced cholestatic index
DILI	drug-induced liver injury
ERA	endothelin receptor antagonist
HBSS	Hank's balanced salt solution
HLMs	human liver microsomes
IC_{50}	half-maximal inhibitory concentration
K_{flux}	first-order rate constant for flux from bile networks into buffer
K_i	inhibition constant
LC_{50}	concentration at the half-maximal toxicity
LCA	lithocholic acid
LRP-1	lipoprotein receptor-related protein-1
MDR/Mdr	multidrug resistance protein
MPA	mycophenolic acid
MRP/Mrp	multidrug resistance-associated protein
NTCP/Ntcp	sodium taurocholate co-transporting polypeptide
OATP/Oatp	organic anion transporting polypeptide
OAT/Oat	organic anion transporter
OCT/Oct	organic cation transporter
P-gp	p-glycoprotein
PI	protease inhibitor
PKC	protein kinase C
PMA	phorbol-12-myristate-13-acetate
PBPK	physiologically-based pharmacokinetic
RSV	rosuvastatin
SCH	sandwich-cultured hepatocytes
SF	scaling factor
TCA	taurocholic acid

TGZ	troglitazone
UDCA	ursodeoxycholic acid

References

1. Swift B, Pfeifer ND, Brouwer KL. Sandwich-cultured hepatocytes: an in vitro model to evaluate hepatobiliary transporter-based drug interactions and hepatotoxicity. Drug Metab Rev. 2010; 42(3): 446–471. [PubMed: 20109035]
2. Borlak J, Klutcka T. Expression of basolateral and canalicular transporters in rat liver and cultures of primary hepatocytes. Xenobiotica. 2004; 34(11–12):935–947. [PubMed: 15801539]
3. Dunn JC, Tompkins RG, Yarmush ML. Long-term in vitro function of adult hepatocytes in a collagen sandwich configuration. Biotechnol Prog. 1991; 7(3):237–245. [PubMed: 1367596]
4. Dunn JC, Tompkins RG, Yarmush ML. Hepatocytes in collagen sandwich: evidence for transcriptional and translational regulation. The Journal of cell biology. 1992; 116(4):1043–1053. [PubMed: 1734019]
5. LeCluyse EL, Audus KL, Hochman JH. Formation of extensive canalicular networks by rat hepatocytes cultured in collagen-sandwich configuration. The American journal of physiology. 1994; 266(6 Pt 1):C1764–1774. [PubMed: 8023906]
6. Liu X, Brouwer KL, Gan LS, Brouwer KR, Stieger B, Meier PJ, Audus KL, LeCluyse EL. Partial maintenance of taurocholate uptake by adult rat hepatocytes cultured in a collagen sandwich configuration. Pharm Res. 1998; 15(10):1533–1539. [PubMed: 9794494]
7. Kotani N, Maeda K, Watanabe T, et al. Culture period-dependent changes in the uptake of transporter substrates in sandwich-cultured rat and human hepatocytes. Drug Metab Dispos. 2011; 39(9):1503–1510. [PubMed: 21673128]
8. Hoffmaster KA, Turncliff RZ, LeCluyse EL, Kim RB, Meier PJ, Brouwer KL. P-glycoprotein expression, localization, and function in sandwich-cultured primary rat and human hepatocytes: relevance to the hepatobiliary disposition of a model opioid peptide. Pharm Res. 2004; 21(7):1294–1302. [PubMed: 15290872]
9. Kimoto E, Yoshida K, Balogh LM, et al. Characterization of organic anion transporting polypeptide (OATP) expression and its functional contribution to the uptake of substrates in human hepatocytes. Mol Pharm. 2012; 9(12):3535–3542. [PubMed: 23082789]
10. Bow DA, Perry JL, Miller DS, Pritchard JB, Brouwer KL. Localization of P-gp (Abcb1) and Mrp2 (Abcc2) in freshly isolated rat hepatocytes. Drug Metab Dispos. 2008; 36(1):198–202. [PubMed: 17954525]
11. Kotani N, Maeda K, Watanabe T, Hiramatsu M, Gong LK, Bi YA, Takezawa T, Kusuhara H, Sugiyama Y. Culture period-dependent changes in the uptake of transporter substrates in sandwich-cultured rat and human hepatocytes. Drug Metab Dispos. 2011; 39(9):1503–1510. [PubMed: 21673128]
12. Tchaparian EH, Houghton JS, Uyeda C, Grillo MP, Jin L. Effect of culture time on the basal expression levels of drug transporters in sandwich-cultured primary rat hepatocytes. Drug Metab Dispos. 2011; 39(12):2387–2394. [PubMed: 21865320]
13. Li N, Singh P, Mandrell KM, Lai Y. Improved extrapolation of hepatobiliary clearance from in vitro sandwich cultured rat hepatocytes through absolute quantification of hepatobiliary transporters. Mol Pharm. 2010; 7(3):630–641. [PubMed: 20438085]
14. Jacobsen JK, Jensen B, Skonberg C, Hansen SH, Badolo L. Time-course activities of Oct1, Mrp3, and cytochrome P450s in cultures of cryopreserved rat hepatocytes. Eur J Pharm Sci. 2011; 44(3): 427–436. [PubMed: 21925601]
15. De Bruyn T, Chatterjee S, Fattah S, et al. Sandwich-cultured hepatocytes: utility for in vitro exploration of hepatobiliary drug disposition and druginduced hepatotoxicity. Expert Opin Drug Metab Toxicol. 2013; 9(5):589–616. [PubMed: 23452081]
16. Godoy P, Hewitt NJ, Albrecht U, et al. Recent advances in 2D and 3D in vitro systems using primary hepatocytes, alternative hepatocyte sources and nonparenchymal liver cells and their use

in investigating mechanisms of hepatotoxicity, cell signaling and ADME. Arch Toxicol. 2013; 87(8):1315–1530. [PubMed: 23974980]

17. Liu X, LeCluyse EL, Brouwer KR, Gan LS, Lemasters JJ, Stieger B, Meier PJ, Brouwer KL. Biliary excretion in primary rat hepatocytes cultured in a collagen-sandwich configuration. Am J Physiol. 1999; 277(1 Pt 1):G12–21. [PubMed: 10409146]
18. Liu X, LeCluyse EL, Brouwer KR, Lightfoot RM, Lee JI, Brouwer KL. Use of Ca2+ modulation to evaluate biliary excretion in sandwich-cultured rat hepatocytes. J Pharmacol Exp Ther. 1999; 289(3):1592–1599. [PubMed: 10336557]
19. Jackson JP, Kabirov KK, Kapetanovic IM, Lyubimov A. In vitro assessment of P450 induction potential of novel chemopreventive agents SR13668, 9-cis-UAB30, and pentamethychromanol in primary cultures of human hepatocytes. Chemico-biological interactions. 2009; 179(2–3):263–272. [PubMed: 19135037]
20. Treijtel N, Barendregt A, Freidig AP, Blaauboer BJ, van Eijkeren JC. Modeling the in vitro intrinsic clearance of the slowly metabolized compound tolbutamide determined in sandwich-cultured rat hepatocytes. Drug Metab Dispos. 2004; 32(8):884–891. [PubMed: 15258115]
21. Treijtel N, van Helvoort H, Barendregt A, Blaauboer BJ, van Eijkeren JC. The use of sandwich-cultured rat hepatocytes to determine the intrinsic clearance of compounds with different extraction ratios: 7-ethoxycoumarin and warfarin. Drug Metab Dispos. 2005; 33(9):1325–1332. [PubMed: 15951450]
22. Generaux CN, Ainslie GR, Bridges AS, et al. Compartmental and enzyme kinetic modeling to elucidate the biotransformation pathway of a centrally acting antitrypanosomal prodrug. Drug Metab Dispos. 2013; 41(2):518–528. [PubMed: 23223498]
23. Shen G, Zhuang X, Xiao W, Kong L, Tan Y, Li H. Role of CYP3A in regulating hepatic clearance and hepatotoxicity of triptolide in rat liver microsomes and sandwich-cultured hepatocytes. Food Chem Toxicol. 2014; 71:90–96. [PubMed: 24910460]
24. Bi YA, Kimoto E, Sevidal S, et al. In vitro evaluation of hepatic transportermediated clinical drug-drug interactions: hepatocyte model optimization and retrospective investigation. Drug Metab Dispos. 2012; 40(6):1085–1092. [PubMed: 22381335]
25. Zhang Z, Farooq M, Prasad B, Grepper S, Unadkat JD. Prediction of gestational age-dependent induction of in vivo hepatic CYP3A activity based on HepaRG cells and human hepatocytes. Drug Metab Dispos. 2015; 43(6):836–842. [PubMed: 25802327]
26. Abe K, Bridges AS, Yue W, Brouwer KL. In vitro biliary clearance of angiotensin II receptor blockers and 3-hydroxy-3-methylglutaryl-coenzyme A reductase inhibitors in sandwich-cultured rat hepatocytes: comparison with in vivo biliary clearance. J Pharmacol Exp Ther. 2008; 326(3): 983–990. [PubMed: 18574002]
27. Zamek-Gliszczynski MJ, Bedwell DW, Bao JQ, Higgins JW. Characterization of SAGE Mdr1a (P-gp), Bcrp, and Mrp2 knockout rats using loperamide, paclitaxel, sulfasalazine, and carboxydichlorofluorescein pharmacokinetics. Drug Metab Dispos. 2012; 40(9):1825–1833. [PubMed: 22711747]
28. Yue W, Abe K, Brouwer KL. Knocking down breast cancer resistance protein (Bcrp) by adenoviral vector-mediated RNA interference (RNAi) in sandwichcultured rat hepatocytes: a novel tool to assess the contribution of Bcrp to drug biliary excretion. Mol Pharm. 2009; 6(1):134–143. [PubMed: 19105722]
29. Yang K, Pfeifer ND, Hardwick RN, Yue W, Stewart PW, Brouwer KL. An experimental approach to evaluate the impact of impaired transport function on hepatobiliary drug disposition using Mrp2-deficient TR- rat sandwichcultured hepatocytes in combination with Bcrp knockdown. Mol Pharm. 2014; 11(3):766–775. [PubMed: 24410402]
30. Lepist EI, Gillies H, Smith W, et al. Evaluation of the endothelin receptor antagonists ambrisentan, bosentan, macitentan, and sitaxsentan as hepatobiliary transporter inhibitors and substrates in sandwich-cultured human hepatocytes. PLoS One. 2014; 9(1):e87548. [PubMed: 24498134]
31. Yanni SB, Augustijns PF, Benjamin DK Jr, Brouwer KL, Thakker DR, Annaert PP. In vitro investigation of the hepatobiliary disposition mechanisms of the antifungal agent micafungin in humans and rats. Drug Metab Dispos. 2010; 38(10):1848–1856. [PubMed: 20606004]

32. Mohamed LA, Kaddoumi A. Tacrine sinusoidal uptake and biliary excretion in sandwich-cultured primary rat hepatocytes. J Pharm Pharm Sci. 2014; 17(3):427–438. [PubMed: 25224352]
33. Sharma S, Ellis EC, Gramignoli R, Dorko K, Tahan V, Hansel M, Mattison DR, Caritis SN, Hines RN, Venkataramanan R, Strom SC. Hepatobiliary disposition of 17-OHPC and taurocholate in fetal human hepatocytes: a comparison with adult human hepatocytes. Drug Metab Dispos. 2013; 41(2):296–304. [PubMed: 23129211]
34. Sheng J, Tian X, Xu G, Wu Z, Chen C, Wang L, Pan L, Huang C, Pan G. The hepatobiliary disposition of timosaponin b2 is highly dependent on influx/efflux transporters but not metabolism. Drug metabolism and disposition: the biological fate of chemicals. 2015; 43(1):63–72. [PubMed: 25336752]
35. Mohamed LA, Kaddoumi A. In vitro investigation of amyloid-beta hepatobiliary disposition in sandwich-cultured primary rat hepatocytes. Drug metabolism and disposition: the biological fate of chemicals. 2013; 41(10):1787–1796. [PubMed: 23852717]
36. Roggenbeck BA, Carew MW, Charrois GJ, Douglas DN, Kneteman NM, Lu X, Le XC, Leslie EM. Characterization of arsenic hepatobiliary transport using sandwich-cultured human hepatocytes. Toxicol Sci. 2015; 145(2):307–320. [PubMed: 25752797]
37. De Bruyn T, Ye ZW, Peeters A, Sahi J, Baes M, Augustijns PF, Annaert PP. Determination of OATP-, NTCP- and OCT-mediated substrate uptake activities in individual and pooled batches of cryopreserved human hepatocytes. Eur J Pharm Sci. 2011; 43(4):297–307. [PubMed: 21605667]
38. Williamson B, Soars AC, Owen A, White P, Riley RJ, Soars MG. Dissecting the relative contribution of OATP1B1-mediated uptake of xenobiotics into human hepatocytes using siRNA. Xenobiotica. 2013; 43(10):920–931. [PubMed: 23461378]
39. Vavricka SR, Van Montfoort J, Ha HR, Meier PJ, Fattinger K. Interactions of rifamycin SV and rifampicin with organic anion uptake systems of human liver. Hepatology. 2002; 36(1):164–172. [PubMed: 12085361]
40. Webborn PJ, Parker AJ, Denton RL, Riley RJ. In vitro-in vivo extrapolation of hepatic clearance involving active uptake: theoretical and experimental aspects. Xenobiotica; the fate of foreign compounds in biological systems. 2007; 37(10–11):1090–1109.
41. Liu X, Chism JP, LeCluyse EL, Brouwer KR, Brouwer KL. Correlation of biliary excretion in sandwich-cultured rat hepatocytes and in vivo in rats. Drug Metab Dispos. 1999; 27(6):637–644. [PubMed: 10348791]
42. Pan G, Boiselle C, Wang J. Assessment of biliary clearance in early drug discovery using sandwich-cultured hepatocyte model. J Pharm Sci. 2012; 101(5):1898–1908. [PubMed: 22323123]
43. Ghibellini G, Vasist LS, Leslie EM, Heizer WD, Kowalsky RJ, Calvo BF, Brouwer KL. In vitro-in vivo correlation of hepatobiliary drug clearance in humans. Clinical pharmacology and therapeutics. 2007; 81(3):406–413. [PubMed: 17235333]
44. Fukuda H, Ohashi R, Tsuda-Tsukimoto M, Tamai I. Effect of plasma protein binding on in vitro-in vivo correlation of biliary excretion of drugs evaluated by sandwich-cultured rat hepatocytes. Drug Metab Dispos. 2008; 36(7):1275–1282. [PubMed: 18388177]
45. Nakakariya M, Ono M, Amano N, Moriwaki T, Maeda K, Sugiyama Y. In vivo biliary clearance should be predicted by intrinsic biliary clearance in sandwich-cultured hepatocytes. Drug Metab Dispos. 2012; 40(3):602–609. [PubMed: 22190695]
46. Ferslew BC, Kock K, Bridges AS, Brouwer KL. Role of multidrug resistance-associated protein 4 in the basolateral efflux of hepatically derived enalaprilat. Drug Metab Dispos. 2014; 42(9):1567–1574. [PubMed: 24958844]
47. Neuvonen PJ, Niemi M, Backman JT. Drug interactions with lipid-lowering drugs: mechanisms and clinical relevance. Clinical pharmacology and therapeutics. 2006; 80(6):565–581. [PubMed: 17178259]
48. Woodhead JL, Yang K, Siler SQ, Watkins PB, Brouwer KLR, Barton HA, BAH. Exploring BSEP inhibition-mediated toxicity with a mechanistic model of drug-induced liver injury. Front Pharmacol. 2014; 5(240)
49. Yang K, Woodhead JL, Watkins PB, Howell BA, Brouwer KL. Systems pharmacology modeling predicts delayed presentation and species differences in bile acid-mediated troglitazone

hepatotoxicity. Clinical pharmacology and therapeutics. 2014; 96(5):589–598. [PubMed: 25068506]

50. Pfeifer ND, Goss SL, Swift B, Ghibellini G, Ivanovic M, Heizer WD, Gangarosa LM, Brouwer KL. Effect of Ritonavir on (99m)Technetium-Mebrofenin Disposition in Humans: A Semi-PBPK Modeling and In Vitro Approach to Predict Transporter-Mediated DDIs. CPT Pharmacometrics Syst Pharmacol. 2013; 2:e20. [PubMed: 23887590]
51. Powell J, Farasyn T, Kock K, Meng X, Pahwa S, Brouwer KL, Yue W. Novel mechanism of impaired function of organic anion-transporting polypeptide 1B3 in human hepatocytes: post-translational regulation of OATP1B3 by protein kinase C activation. Drug Metab Dispos. 2014; 42(11):1964–1970. [PubMed: 25200870]
52. Kruglov EA, Gautam S, Guerra MT, Nathanson MH. Type 2 inositol 1,4,5-trisphosphate receptor modulates bile salt export pump activity in rat hepatocytes. Hepatology. 2011; 54(5):1790–1799. [PubMed: 21748767]
53. Draheim V, Reichel A, Weitschies W, Moenning U. N-glycosylation of ABC transporters is associated with functional activity in sandwich-cultured rat hepatocytes. Eur J Pharm Sci. 2010; 41(2):201–209. [PubMed: 20558284]
54. Zhang P, Tian X, Chandra P, Brouwer KL. Role of glycosylation in trafficking of Mrp2 in sandwich-cultured rat hepatocytes. Molecular pharmacology. 2005; 67(4):1334–1341. [PubMed: 15662046]
55. Noel G, Le Vee M, Moreau A, Stieger B, Parmentier Y, Fardel O. Functional expression and regulation of drug transporters in monolayer- and sandwich-cultured mouse hepatocytes. Eur J Pharm Sci. 2013; 49(1):39–50. [PubMed: 23396053]
56. Jackson JP, Taylor R, Rajaraman G, Easterwood L, Hill J, Baucom C, Ferguson S. Induction of Transporter Expression and Modulation of Hepatobiliary Disposition using Sandwich Cultures of Human Hepatocytes. ISSX Online Abstracts, Supplement. 2014; 9(2):P364.
57. Fukuda H, Nakanishi T, Tamai I. More relevant prediction for in vivo drug interaction of candesartan cilexetil on hepatic bile acid transporter BSEP using sandwich-cultured hepatocytes. Drug Metab Pharmacokinet. 2014; 29(1):94–96. [PubMed: 23877105]
58. Yang K, Brouwer KL. Hepatocellular exposure of troglitazone metabolites in rat sandwich-cultured hepatocytes lacking Bcrp and Mrp2: interplay between formation and excretion. Drug metabolism and disposition: the biological fate of chemicals. 2014; 42(7):1219–1226. [PubMed: 24799397]
59. Nakanishi T, Ikenaga M, Fukuda H, Matsunaga N, Tamai I. Application of quantitative time-lapse imaging (QTLI) for evaluation of Mrp2-based drug-drug interaction induced by liver metabolites. Toxicol Appl Pharmacol. 2012; 263(2):244–250. [PubMed: 22766462]
60. Jones HM, Barton HA, Lai Y, Bi YA, Kimoto E, Kempshall S, Tate SC, El-Kattan A, Houston JB, Galetin A, Fenner KS. Mechanistic pharmacokinetic modeling for the prediction of transporter-mediated disposition in humans from sandwich culture human hepatocyte data. Drug Metab Dispos. 2012; 40(5):1007–1017. [PubMed: 22344703]
61. Li R, Ghosh A, Maurer TS, Kimoto E, Barton HA. Physiologically based pharmacokinetic prediction of telmisartan in human. Drug metabolism and disposition: the biological fate of chemicals. 2014; 42(10):1646–1655. [PubMed: 25092714]
62. Jones HM, Mayawala K, Poulin P. Dose selection based on physiologically based pharmacokinetic (PBPK) approaches. Aaps j. 2013; 15(2):377–387. [PubMed: 23269526]
63. Oshio C, Phillips MJ. Contractility of bile canaliculi: implications for liver function. Science. 1981; 212(4498):1041–1042. [PubMed: 7015506]
64. Phillips MJ, Oshio C, Miyairi M, Katz H, Smith CR. A study of bile canalicular contractions in isolated hepatocytes. Hepatology. 1982; 2(6):763–768. [PubMed: 7141386]
65. Boyer JL, Gautam A, Graf J. Mechanisms of bile secretion: insights from the isolated rat hepatocyte couplet. Semin Liver Dis. 1988; 8(4):308–316. [PubMed: 2850606]
66. Lee JK, Marion TL, Abe K, Lim C, Pollock GM, Brouwer KL. Hepatobiliary disposition of troglitazone and metabolites in rat and human sandwich-cultured hepatocytes: use of Monte Carlo simulations to assess the impact of changes in biliary excretion on troglitazone sulfate accumulation. J Pharmacol Exp Ther. 2010; 332(1):26–34. [PubMed: 19801447]

67. Pfeifer ND, Yang K, Brouwer KL. Hepatic basolateral efflux contributes significantly to rosuvastatin disposition I: characterization of basolateral versus biliary clearance using a novel protocol in sandwich-cultured hepatocytes. J Pharmacol Exp Ther. 2013; 347(3):727–736. [PubMed: 24023367]

68. Yang K, Pfeifer ND, Kock K, Brouwer KL. Species Differences in Hepatobiliary Disposition of Taurocholic Acid in Human and Rat Sandwich-Cultured Hepatocytes: Implications for Drug-Induced Liver Injury. J Pharmacol Exp Ther. 2015

69. Guo C, Brouwer KR, Yang K, St Claire R, Brouwer KLR. Prediction of altered bile acid disposition by drugs using an integrated approach: Sandwich-cultured human hepatocytes, mechanistic modeling and simulation. ISSX Online Abstracts Supplement. 2014; 9(2):P534.

70. Menochet K, Kenworthy KE, Houston JB, Galetin A. Simultaneous assessment of uptake and metabolism in rat hepatocytes: a comprehensive mechanistic model. J Pharmacol Exp Ther. 2012; 341(1):2–15. [PubMed: 22190645]

71. Houston JB. Utility of in vitro drug metabolism data in predicting in vivo metabolic clearance. Biochem Pharmacol. 1994; 47(9):1469–1479. [PubMed: 8185657]

72. Poulin P, Haddad S. Toward a new paradigm for the efficient in vitro-in vivo extrapolation of metabolic clearance in humans from hepatocyte data. J Pharm Sci. 2013; 102(9):3239–3251. [PubMed: 23494893]

73. Jones HM, Barton HA, Lai Y, Bi YA, Kimoto E, Kempshall S, Tate SC, El-Kattan A, Houston JB, Galetin A, Fenner KS. Mechanistic pharmacokinetic modeling for the prediction of transporter-mediated disposition in humans from sandwich culture human hepatocyte data. Drug metabolism and disposition: the biological fate of chemicals. 2012; 40(5):1007–1017. [PubMed: 22344703]

74. Varma MV, Scialis RJ, Lin J, Bi YA, Rotter CJ, Goosen TC, Yang X. Mechanism-based pharmacokinetic modeling to evaluate transporter-enzyme interplay in drug interactions and pharmacogenetics of glyburide. The AAPS journal. 2014; 16(4):736–748. [PubMed: 24839071]

75. Varma MV, Lai Y, Feng B, Litchfield J, Goosen TC, Bergman A. Physiologically based modeling of pravastatin transporter-mediated hepatobiliary disposition and drug-drug interactions. Pharmaceutical research. 2012; 29(10):2860–2873. [PubMed: 22638872]

76. Varma MV, Lin J, Bi YA, Rotter CJ, Fahmi OA, Lam J, El-Kattan AF, Goosen TC, Lai Y. Quantitative Prediction of Repaglinide-Rifampicin Complex Drug Interactions Using Dynamic and Static Mechanistic Models: Delineating Differential CYP3A4 Induction and OATP1B1 Inhibition Potential of Rifampicin. Drug metabolism and disposition: the biological fate of chemicals. 2013

77. Varma MV, Scialis RJ, Lin J, Bi YA, Rotter CJ, Goosen TC, Yang X. Mechanism-based pharmacokinetic modeling to evaluate transporter-enzyme interplay in drug interactions and pharmacogenetics of glyburide. The AAPS journal. 2014; 16(4):736–748. [PubMed: 24839071]

78. Li R, Barton HA, Yates PD, Ghosh A, Wolford AC, Riccardi KA, Maurer TS. A “middle-out” approach to human pharmacokinetic predictions for OATP substrates using physiologically-based pharmacokinetic modeling. Journal of pharmacokinetics and pharmacodynamics. 2014; 41(3): 197–209. [PubMed: 24718648]

79. Agarwal S, Uchida Y, Mittapalli RK, Sane R, Terasaki T, Elmquist WF. Quantitative proteomics of transporter expression in brain capillary endothelial cells isolated from P-glycoprotein (P-gp), breast cancer resistance protein (Bcrp), and P-gp/Bcrp knockout mice. Drug metabolism and disposition: the biological fate of chemicals. 2012; 40(6):1164–1169. [PubMed: 22401960]

80. Shawahna R, Uchida Y, Decleves X, Ohtsuki S, Yousif S, Dauchy S, Jacob A, Chassoux F, Daumas-Duport C, Couraud PO, Terasaki T, Scherrmann JM. Transcriptomic and quantitative proteomic analysis of transporters and drug metabolizing enzymes in freshly isolated human brain microvessels. Molecular pharmaceutics. 2011; 8(4):1332–1341. [PubMed: 21707071]

81. Uchida Y, Tachikawa M, Obuchi W, Hoshi Y, Tomioka Y, Ohtsuki S, Terasaki T. A study protocol for quantitative targeted absolute proteomics (QTAP) by LC-MS/MS: application for inter-strain differences in protein expression levels of transporters, receptors, claudin-5, and marker proteins at the blood-brain barrier in ddY, FVB, and C57BL/6J mice. Fluids and barriers of the CNS. 2013; 10(1):21. [PubMed: 23758935]

82. Sakamoto A, Matsumaru T, Yamamura N, Uchida Y, Tachikawa M, Ohtsuki S, Terasaki T. Quantitative expression of human drug transporter proteins in lung tissues: analysis of regional,

gender, and interindividual differences by liquid chromatography-tandem mass spectrometry. J Pharm Sci. 2013; 102(9):3395–3406. [PubMed: 23670800]

83. Sakamoto A, Matsumaru T, Yamamura N, Suzuki S, Uchida Y, Tachikawa M, Terasaki T. Drug Transporter Protein Quantification of Immortalized Human Lung Cell Lines Derived from Tracheobronchial Epithelial Cells (Calu-3 and BEAS2-B), Bronchiolar-Alveolar Cells (NCI-H292 and NCI-H441), and Alveolar Type II-like Cells (A549) by Liquid Chromatography-Tandem Mass Spectrometry. J Pharm Sci. 2015; 104(9):3029–3038. [PubMed: 25690838]
84. Li N, Bi YA, Duignan DB, Lai Y. Quantitative expression profile of hepatobiliary transporters in sandwich cultured rat and human hepatocytes. Molecular pharmaceutics. 2009; 6(4):1180–1189. [PubMed: 19545175]
85. Vildhede A, Wisniewski JR, Noren A, Karlgren M, Artursson P. Comparative Proteomic Analysis of Human Liver Tissue and Isolated Hepatocytes with a Focus on Proteins Determining Drug Exposure. Journal of proteome research. 2015; 14(8):3305–3314. [PubMed: 26167961]
86. Badee J, Achour B, Rostami-Hodjegan A, Galetin A. Meta-analysis of expression of hepatic organic anion-transporting polypeptide (OATP) transporters in cellular systems relative to human liver tissue. Drug metabolism and disposition: the biological fate of chemicals. 2015; 43(4):424–432. [PubMed: 25564656]
87. Jamei M, Marciniak S, Feng K, Barnett A, Tucker G, Rostami-Hodjegan A. The Simcyp population-based ADME simulator. Expert opinion on drug metabolism & toxicology. 2009; 5(2): 211–223. [PubMed: 19199378]
88. Wilkinson GR. Clearance approaches in pharmacology. Pharmacol Rev. 1987; 39(1):1–47. [PubMed: 3554275]
89. Varma MV, Lai Y, Feng B, Litchfield J, Goosen TC, Bergman A. Physiologically based modeling of pravastatin transporter-mediated hepatobiliary disposition and drug-drug interactions. Pharm Res. 2012; 29(10):2860–2873. [PubMed: 22638872]
90. Jamei M, Bajot F, Neuhoff S, Barter Z, Yang J, Rostami-Hodjegan A, Rowland-Yeo K. A mechanistic framework for in vitro-in vivo extrapolation of liver membrane transporters: prediction of drug-drug interaction between rosuvastatin and cyclosporine. Clinical pharmacokinetics. 2014; 53(1):73–87. [PubMed: 23881596]
91. Yan GZ, Generaux CN, Yoon M, Goldsmith RB, Tidwell RR, Hall JE, Olson CA, Clewell HJ, Brouwer KL, Paine MF. A semiphysiologically based pharmacokinetic modeling approach to predict the dose-exposure relationship of an antiparasitic prodrug/active metabolite pair. Drug Metab Dispos. 2012; 40(1):6–17. [PubMed: 21953913]
92. Li R, Barton HA, Varma MV. Prediction of pharmacokinetics and drug-drug interactions when hepatic transporters are involved. Clinical pharmacokinetics. 2014; 53(8):659–678. [PubMed: 25056496]
93. Varma MV, Lai Y, Kimoto E, Goosen TC, El-Kattan AF, Kumar V. Mechanistic modeling to predict the transporter- and enzyme-mediated drug-drug interactions of repaglinide. Pharm Res. 2013; 30(4):1188–1199. [PubMed: 23307347]
94. Lee WM. Drug-induced hepatotoxicity. N Engl J Med. 2003; 349(5):474–485. [PubMed: 12890847]
95. FDA Guidance for Industry Drug-Induced Liver Injury: Premarketing Clinical Evaluation. 2009
96. Abboud G, Kaplowitz N. Drug-induced liver injury. Drug Saf. 2007; 30(4):277–294. [PubMed: 17408305]
97. Thompson RA, Isin EM, Li Y, Weidolf L, Page K, Wilson I, Swallow S, Middleton B, Stahl S, Foster AJ, Dolgos H, Weaver R, Kenna JG. In vitro approach to assess the potential for risk of idiosyncratic adverse reactions caused by candidate drugs. Chem Res Toxicol. 2012; 25(8):1616–1632. [PubMed: 22646477]
98. Parmentier C, Truisi GL, Moenks K, Stanzel S, Lukas A, Kopp-Schneider A, Alexandre E, Hewitt PG, Mueller SO, Richert L. Transcriptomic hepatotoxicity signature of chlorpromazine after short- and long-term exposure in primary human sandwich cultures. Drug metabolism and disposition: the biological fate of chemicals. 2013; 41(10):1835–1842. [PubMed: 23913027]

99. Surendradoss J, Chang TK, Abbott FS. Assessment of the role of in situ generated (E)-2,4-diene-valproic acid in the toxicity of valproic acid and (E)-2-ene-valproic acid in sandwich-cultured rat hepatocytes. Toxicology and applied pharmacology. 2012; 264(3):413–422. [PubMed: 22940460]
100. Dong JQ, Smith PC. Glucuronidation and covalent protein binding of benoxaprofen and flunoxaprofen in sandwich-cultured rat and human hepatocytes. Drug metabolism and disposition: the biological fate of chemicals. 2009; 37(12):2314–2322. [PubMed: 19773537]
101. Perez MJ, Briz O. Bile-acid-induced cell injury and protection. World J Gastroenterol. 2009; 15(14):1677–1689. [PubMed: 19360911]
102. Maillette de Buy Wenniger L, Beuers U. Bile salts and cholestasis. Dig Liver Dis. 2010; 42(6): 409–418. [PubMed: 20434968]
103. Morgan RE, van Staden CJ, Chen Y, Kalyanaraman N, Kalanzi J, Dunn RT 2nd, Afshari CA, Hamadeh HK. A Multifactorial Approach to Hepatobiliary Transporter Assessment Enables Improved Therapeutic Compound Development. Toxicol Sci. 2013
104. Dawson S, Stahl S, Paul N, Barber J, Kenna JG. In vitro inhibition of the bile salt export pump correlates with risk of cholestatic drug-induced liver injury in humans. Drug Metab Dispos. 2012; 40(1):130–138. [PubMed: 21965623]
105. Kock K, Ferslew BC, Netterberg I, Yang K, Urban TJ, Swaan PW, Stewart PW, Brouwer KL. Risk Factors for Development of Cholestatic Drug-induced Liver Injury: Inhibition of Hepatic Basolateral Bile Acid Transporters MRP3 and MRP4. Drug Metab Dispos. 2013
106. Pedersen JM, Matsson P, Bergstrom CA, Hoogstraate J, Noren A, Lecluyse EL, Artursson P. Early Identification of Clinically Relevant Drug Interactions With the Human Bile Salt Export Pump (BSEP/ABCB11). Toxicol Sci. 2013; 136(2):328–343. [PubMed: 24014644]
107. Hofmann AF. Bile Acids: The Good, the Bad, and the Ugly. News Physiol Sci. 1999; 14:24–29. [PubMed: 11390813]
108. Thomas C, Pellicciari R, Pruzanski M, Auwerx J, Schoonjans K. Targeting bile-acid signalling for metabolic diseases. Nat Rev Drug Discov. 2008; 7(8):678–693. [PubMed: 18670431]
109. Scholmerich J, Becher MS, Schmidt K, Schubert R, Kremer B, Feldhaus S, Gerok W. Influence of hydroxylation and conjugation of bile salts on their membrane-damaging properties--studies on isolated hepatocytes and lipid membrane vesicles. Hepatology. 1984; 4(4):661–666. [PubMed: 6745854]
110. Yang K, Kock K, Sedykh A, Tropsha A, Brouwer KL. An updated review on drug-induced cholestasis: mechanisms and investigation of physicochemical properties and pharmacokinetic parameters. J Pharm Sci. 2013; 102(9):3037–3057. [PubMed: 23653385]
111. Trauner M, Boyer JL. Bile salt transporters: molecular characterization, function, and regulation. Physiol Rev. 2003; 83(2):633–671. [PubMed: 12663868]
112. Dawson PA, Lan T, Rao A. Bile acid transporters. J Lipid Res. 2009; 50(12):2340–2357. [PubMed: 19498215]
113. Chiang JY. Bile acids: regulation of synthesis. J Lipid Res. 2009; 50(10):1955–1966. [PubMed: 19346330]
114. Marion TL, Perry CH, St Claire RL 3rd, Brouwer KL. Endogenous bile acid disposition in rat and human sandwich-cultured hepatocytes. Toxicol Appl Pharmacol. 2012; 261(1):1–9. [PubMed: 22342602]
115. Akita H, Suzuki H, Sugiyama Y. Sinusoidal efflux of taurocholate is enhanced in Mrp2-deficient rat liver. Pharm Res. 2001; 18(8):1119–1125. [PubMed: 11587482]
116. Trauner M, Wagner M, Fickert P, Zollner G. Molecular regulation of hepatobiliary transport systems: clinical implications for understanding and treating cholestasis. J Clin Gastroenterol. 2005; 39(4 Suppl 2):S111–124. [PubMed: 15758646]
117. Zollner G, Wagner M, Fickert P, Silbert D, Gumhold J, Zatloukal K, Denk H, Trauner M. Expression of bile acid synthesis and detoxification enzymes and the alternative bile acid efflux pump MRP4 in patients with primary biliary cirrhosis. Liver Int. 2007; 27(7):920–929. [PubMed: 17696930]
118. Ballatori N, Li N, Fang F, Boyer JL, Christian WV, Hammond CL. OST alpha-OST beta: a key membrane transporter of bile acids and conjugated steroids. Front Biosci. 2009; 14:2829–2844.

119. Yang K, Pfeifer ND, Kock K, Brouwer KL. Species differences in hepatobiliary disposition of taurocholic acid in human and rat sandwich-cultured hepatocytes: implications for drug-induced liver injury. The Journal of pharmacology and experimental therapeutics. 2015; 353(2):415–423. [PubMed: 25711339]

120. van de Steeg E, Stranecky V, Hartmannova H, Noskova L, Hrebicek M, Wagenaar E, van Esch A, de Waart DR, Oude Elferink RP, Kenworthy KE, Sticova E, al-Edreesi M, Knisely AS, Kmoch S, Jirsa M, Schinkel AH. Complete OATP1B1 and OATP1B3 deficiency causes human Rotor syndrome by interrupting conjugated bilirubin reuptake into the liver. The Journal of clinical investigation. 2012; 122(2):519–528. [PubMed: 22232210]

121. Sharma S, Ellis EC, Gramignoli R, Dorko K, Tahan V, Hansel M, Mattison DR, Caritis SN, Hines RN, Venkataramanan R, Strom SC. Hepatobiliary disposition of 17-OHPC and taurocholate in fetal human hepatocytes: a comparison with adult human hepatocytes. Drug metabolism and disposition: the biological fate of chemicals. 2013; 41(2):296–304. [PubMed: 23129211]

122. Morgan RE, Trauner M, van Staden CJ, Lee PH, Ramachandran B, Eschenberg M, Afshari CA, Qualls CW Jr, Lightfoot-Dunn R, Hamadeh HK. Interference with bile salt export pump function is a susceptibility factor for human liver injury in drug development. Toxicol Sci. 2010; 118(2): 485–500. [PubMed: 20829430]

123. Galie N, Hoeper MM, Gibbs JS, Simonneau G. Liver toxicity of sitaxentan in pulmonary arterial hypertension. The European respiratory journal. 2011; 37(2):475–476. [PubMed: 21282816]

124. Rubin LJ, Badesch DB, Barst RJ, Galie N, Black CM, Keogh A, Pulido T, Frost A, Roux S, Leconte I, Landzberg M, Simonneau G. Bosentan therapy for pulmonary arterial hypertension. N Engl J Med. 2002; 346(12):896–903. [PubMed: 11907289]

125. Humbert M, Segal ES, Kiely DG, Carlsen J, Schwierin B, Hoeper MM. Results of European post-marketing surveillance of bosentan in pulmonary hypertension. The European respiratory journal. 2007; 30(2):338–344. [PubMed: 17504794]

126. Fattinger K, Funk C, Pantze M, Weber C, Reichen J, Stieger B, Meier PJ. The endothelin antagonist bosentan inhibits the canalicular bile salt export pump: a potential mechanism for hepatic adverse reactions. Clin Pharmacol Ther. 2001; 69(4):223–231. [PubMed: 11309550]

127. Kenna JG, Stahl SH, Eakins JA, Foster AJ, Andersson LC, Bergare J, Billger M, Elebring M, Elmore CS, Thompson RA. Multiple compound-related adverse properties contribute to liver injury caused by endothelin receptor antagonists. The Journal of pharmacology and experimental therapeutics. 2015; 352(2):281–290. [PubMed: 25467130]

128. Galie N, Olschewski H, Oudiz RJ, Torres F, Frost A, Ghofrani HA, Badesch DB, McGoon MD, McLaughlin VV, Roecker EB, Gerber MJ, Dufton C, Wiens BL, Rubin LJ. Ambrisentan for the treatment of pulmonary arterial hypertension: results of the ambrisentan in pulmonary arterial hypertension, randomized, double-blind, placebo-controlled, multicenter, efficacy (ARIES) study 1 and 2. Circulation. 2008; 117(23):3010–3019. [PubMed: 18506008]

129. Oudiz RJ, Galie N, Olschewski H, Torres F, Frost A, Ghofrani HA, Badesch DB, McGoon MD, McLaughlin VV, Roecker EB, Harrison BC, Despain D, Dufton C, Rubin LJ. Long-term ambrisentan therapy for the treatment of pulmonary arterial hypertension. J Am Coll Cardiol. 2009; 54(21):1971–1981. [PubMed: 19909879]

130. Sidharta PN, van Giersbergen PL, Halabi A, Dingemanse J. Macitentan: entry-into-humans study with a new endothelin receptor antagonist. European journal of clinical pharmacology. 2011; 67(10):977–984. [PubMed: 21541781]

131. Hartman JC, Brouwer K, Mandagere A, Melvin L, Gorczynski R. Evaluation of the endothelin receptor antagonists ambrisentan, darusentan, bosentan, and sitaxsentan as substrates and inhibitors of hepatobiliary transporters in sandwich-cultured human hepatocytes. Can J Physiol Pharmacol. 2010; 88(6):682–691. [PubMed: 20628435]

132. Sulkowski MS. Drug-induced liver injury associated with antiretroviral therapy that includes HIV-1 protease inhibitors. Clin Infect Dis. 2004; 38(Suppl 2):S90–97. [PubMed: 14986280]

133. Sulkowski MS, Thomas DL, Chaisson RE, Moore RD. Elevated liver enzymes following initiation of antiretroviral therapy. JAMA. 2000; 283(19):2526–2527. [PubMed: 10815113]

134. Bongiovanni M, Cicconi P, Landonio S, Meraviglia P, Testa L, Di Biagio A, Chiesa E, Tordato F, Bini T, Monforte A. Predictive factors of lopinavir/ritonavir discontinuation for drug-related

toxicity: results from a cohort of 416 multi-experienced HIV-infected individuals. Int J Antimicrob Agents. 2005; 26(1):88–91. [PubMed: 15878262]

135. McRae M, Rezk NL, Bridges AS, Corbett AH, Tien HC, Brouwer KL, Kashuba AD. Plasma bile acid concentrations in patients with human immunodeficiency virus infection receiving protease inhibitor therapy: possible implications for hepatotoxicity. Pharmacotherapy. 2010; 30(1):17–24. [PubMed: 20030469]
136. Griffin LM, Watkins PB, Perry CH, St Claire RL 3rd, Brouwer KL. Combination lopinavir and ritonavir alter exogenous and endogenous bile acid disposition in sandwich-cultured rat hepatocytes. Drug metabolism and disposition: the biological fate of chemicals. 2013; 41(1):188–196. [PubMed: 23091188]
137. Li X, Zhong K, Guo Z, Zhong D, Chen X. Fasiglifam (TAK-875) Inhibits Hepatobiliary Transporters: A Possible Factor Contributing to Fasiglifam-induced Liver Injury. Drug metabolism and disposition: the biological fate of chemicals. 2015
138. Guo C, He L, Yao D, AJ, Cao B, Ren J, Wang G, Pan G. Alpha-naphthylisothiocyanate modulates hepatobiliary transporters in sandwich-cultured rat hepatocytes. Toxicol Lett. 2014; 224(1):93–100. [PubMed: 24120425]
139. Marion TL, Leslie EM, Brouwer KL. Use of sandwich-cultured hepatocytes to evaluate impaired bile acid transport as a mechanism of drug-induced hepatotoxicity. Molecular pharmaceutics. 2007; 4(6):911–918. [PubMed: 17963355]
140. Ansede JH, Smith WR, Perry CH, St Claire RL 3rd, Brouwer KR. An in vitro assay to assess transporter-based cholestatic hepatotoxicity using sandwich-cultured rat hepatocytes. Drug Metab Dispos. 2010; 38(2):276–280. [PubMed: 19910518]
141. Kemp DC, Zamek-Gliszczynski MJ, Brouwer KL. Xenobiotics inhibit hepatic uptake and biliary excretion of taurocholate in rat hepatocytes. Toxicol Sci. 2005; 83(2):207–214. [PubMed: 15509663]
142. Funk C, Ponelle C, Scheuermann G, Pantze M. Cholestatic potential of troglitazone as a possible factor contributing to troglitazone-induced hepatotoxicity: in vivo and in vitro interaction at the canalicular bile salt export pump (Bsep) in the rat. Mol Pharmacol. 2001; 59(3):627–635. [PubMed: 11179459]
143. Chatterjee S, Richert L, Augustijns P, Annaert P. Hepatocyte-based in vitro model for assessment of drug-induced cholestasis. Toxicology and applied pharmacology. 2014; 274(1):124–136. [PubMed: 24211272]
144. Trottier J, Caron P, Straka RJ, Barbier O. Profile of serum bile acids in noncholestatic volunteers: gender-related differences in response to fenofibrate. Clin Pharmacol Ther. 2011; 90(2):279–286. [PubMed: 21716269]
145. Mita S, Suzuki H, Akita H, Hayashi H, Onuki R, Hofmann AF, Sugiyama Y. Inhibition of bile acid transport across Na+/taurocholate cotransporting polypeptide (SLC10A1) and bile salt export pump (ABCB 11)-coexpressing LLC-PK1 cells by cholestasis-inducing drugs. Drug metabolism and disposition: the biological fate of chemicals. 2006; 34(9):1575–1581. [PubMed: 16760228]
146. Ye ZW, Van Pelt J, Camus S, Snoeys J, Augustijns P, Annaert P. Species-specific interaction of HIV protease inhibitors with accumulation of cholyl-glycylamido-fluorescein (CGamF) in sandwich-cultured hepatocytes. Journal of pharmaceutical sciences. 2010; 99(6):2886–2898. [PubMed: 20014428]
147. Barber JA, Stahl SH, Summers C, Barrett G, Park BK, Foster JR, Kenna JG. Quantification of drug induced inhibition of canalicular cholyl-l-lysyl-fluorescein excretion from hepatocytes by high content cell imaging. Toxicological sciences : an official journal of the Society of Toxicology. 2015
148. de Waart DR, Hausler S, Vlaming ML, Kunne C, Hanggi E, Gruss HJ, Oude Elferink RP, Stieger B. Hepatic transport mechanisms of cholyl-L-lysyl-fluorescein. The Journal of pharmacology and experimental therapeutics. 2010; 334(1):78–86. [PubMed: 20388726]
149. De Bruyn T, Sempels W, Snoeys J, Holmstock N, Chatterjee S, Stieger B, Augustijns P, Hofkens J, Mizuno H, Annaert P. Confocal imaging with a fluorescent bile acid analogue closely mimicking hepatic taurocholate disposition. Journal of pharmaceutical sciences. 2014; 103(6): 1872–1881. [PubMed: 24652646]

150. Howell BA, Siler SQ, Watkins PB. Use of a systems model of drug-induced liver injury (DILIsym((R))) to elucidate the mechanistic differences between acetaminophen and its less-toxic isomer, AMAP, in mice. Toxicol Lett. 2014; 226(2):163–172. [PubMed: 24560604]

151. Shoda LK, Woodhead JL, Siler SQ, Watkins PB, Howell BA. Linking physiology to toxicity using DILIsym((R)), a mechanistic mathematical model of drug-induced liver injury. Biopharm Drug Dispos. 2014; 35(1):33–49. [PubMed: 24214486]

152. Woodhead JL, Howell BA, Yang Y, Harrill AH, Clewell HJ 3rd, Andersen ME, Siler SQ, Watkins PB. An analysis of N-acetylcysteine treatment for acetaminophen overdose using a systems model of drug-induced liver injury. J Pharmacol Exp Ther. 2012; 342(2):529–540. [PubMed: 22593093]

153. Woodhead JL, Yang K, Brouwer KL, Siler SQ, Stahl SH, Ambroso JL, Baker D, Watkins PB, Howell BA. Mechanistic Modeling Reveals the Critical Knowledge Gaps in Bile Acid-Mediated DILI. CPT: pharmacometrics & systems pharmacology. 2014; 3:e123. [PubMed: 25006780]

154. Ogimura E, Sekine S, Horie T. Bile salt export pump inhibitors are associated with bile acid-dependent drug-induced toxicity in sandwich-cultured hepatocytes. Biochem Biophys Res Commun. 2011; 416(3–4):313–317. [PubMed: 22108051]

155. Ohta M, Kanai S, Kitani K. The order of hepatic cytotoxicity of bile salts in vitro does not agree with that examined in vivo in rats. Life Sci. 1990; 46(21):1503–1508. [PubMed: 2355795]

156. Lee JK, Brouwer KR. Determination of intracellular volume of rat and human sandwich-cultured hepatocytes (Abstract ID 1595). The Toxicologist, Supplement to Toxicological Sciences. 2010; 114(339)

157. Yousef IM, Bouchard G, Tuchweber B, Plaa GL. Monohydroxy bile acid induced cholestasis: role of biotransformation. Drug Metab Rev. 1997; 29(1–2):167–181. [PubMed: 9187517]

158. Hofmann AF. Detoxification of lithocholic acid, a toxic bile acid: relevance to drug hepatotoxicity. Drug Metab Rev. 2004; 36(3–4):703–722. [PubMed: 15554243]

159. Garcia-Canaveras JC, Donato MT, Castell JV, Lahoz A. Targeted profiling of circulating and hepatic bile acids in human, mouse, and rat using a UPLC-MRM-MS-validated method. J Lipid Res. 2012; 53(10):2231–2241. [PubMed: 22822028]

160. Xiang X, Backman JT, Neuvonen PJ, Niemi M. Gender, but not CYP7A1 or SLCO1B1 polymorphism, affects the fasting plasma concentrations of bile acids in human beings. Basic Clin Pharmacol Toxicol. 2012; 110(3):245–252. [PubMed: 21902813]

161. Yang L, Xiong A, He Y, Wang Z, Wang C, Li W, Hu Z. Bile acids metabonomic study on the CCl4- and alpha-naphthylisothiocyanate-induced animal models: quantitative analysis of 22 bile acids by ultraperformance liquid chromatography-mass spectrometry. Chem Res Toxicol. 2008; 21(12):2280–2288. [PubMed: 19053324]

162. Woodhead JL, Yang K, Siler SQ, Watkins PB, Brouwer KL, Barton HA, Howell BA. Exploring BSEP inhibition-mediated toxicity with a mechanistic model of drug-induced liver injury. Frontiers in Pharmacology. 2014; 5:240. [PubMed: 25426072]

163. Yang K, Woodhead JL, Watkins PB, Howell BA, Brouwer KL. Systems pharmacology modeling predicts delayed presentation and species differences in bile acid-mediated troglitazone hepatotoxicity. Clinical pharmacology and therapeutics. 2014; 96(5):589–598. [PubMed: 25068506]

164. Kakis G, Yousef IM. Pathogenesis of lithocholate- and taurolithocholate-induced intrahepatic cholestasis in rats. Gastroenterology. 1978; 75(4):595–607. [PubMed: 213342]

165. Oelberg DG, Chari MV, Little JM, Adcock EW, Lester R. Lithocholate glucuronide is a cholestatic agent. J Clin Invest. 1984; 73(6):1507–1514. [PubMed: 6547150]

166. Yousef IM, Tuchweber B, Vonk RJ, Masse D, Audet M, Roy CC. Lithocholate cholestasis--sulfated glycolithocholate-induced intrahepatic cholestasis in rats. Gastroenterology. 1981; 80(2): 233–241. [PubMed: 7450414]

167. Sokol RJ, Dahl R, Devereaux MW, Yerushalmi B, Kobak GE, Gumpricht E. Human hepatic mitochondria generate reactive oxygen species and undergo the permeability transition in response to hydrophobic bile acids. J Pediatr Gastroenterol Nutr. 2005; 41(2):235–243. [PubMed: 16056106]

168. Faubion WA, Guicciardi ME, Miyoshi H, Bronk SF, Roberts PJ, Svingen PA, Kaufmann SH, Gores GJ. Toxic bile salts induce rodent hepatocyte apoptosis via direct activation of Fas. J Clin Invest. 1999; 103(1):137–145. [PubMed: 9884343]

169. Woolbright BL, Dorko K, Antoine DJ, Clarke JI, Gholami P, Li F, Kumer SC, Schmitt TM, Forster J, Fan F, Jenkins RE, Park BK, Hagenbuch B, Olyaee M, Jaeschke H. Bile acid-induced necrosis in primary human hepatocytes and in patients with obstructive cholestasis. Toxicology and applied pharmacology. 2015; 283(3):168–177. [PubMed: 25636263]

170. Setchell KD, Rodrigues CM, Clerici C, Solinas A, Morelli A, Gartung C, Boyer J. Bile acid concentrations in human and rat liver tissue and in hepatocyte nuclei. Gastroenterology. 1997; 112(1):226–235. [PubMed: 8978363]

171. Leslie EM, Watkins PB, Kim RB, Brouwer KL. Differential inhibition of rat and human Na+-dependent taurocholate cotransporting polypeptide (NTCP/SLC10A1)by bosentan: a mechanism for species differences in hepatotoxicity. J Pharmacol Exp Ther. 2007; 321(3):1170–1178. [PubMed: 17374746]

172. Matsunaga N, Suzuki K, Nakanishi T, Ogawa M, Imawaka H, Tamai I. Modeling approach for multiple transporters-mediated drug-drug interactions in sandwich-cultured human hepatocytes: effect of cyclosporin A on hepatic disposition of mycophenolic acid phenyl-glucuronide. Drug Metab Pharmacokinet. 2015; 30(2):142–148. [PubMed: 25989889]

173. Persson M, Loye AF, Jacquet M, Mow NS, Thougaard AV, Mow T, Hornberg JJ. High-content analysis/screening for predictive toxicology: application to hepatotoxicity and genotoxicity. Basic & clinical pharmacology & toxicology. 2014; 115(1):18–23. [PubMed: 24461077]

174. Ferslew BC, Brouwer KL. Identification of hepatic phospholipidosis inducers in sandwich-cultured rat hepatocytes, a physiologically relevant model, reveals altered basolateral uptake and biliary excretion of anionic probe substrates. Toxicological sciences : an official journal of the Society of Toxicology. 2014; 139(1):99–107. [PubMed: 24563379]

175. He L, Yang Y, Guo C, Yao D, Liu HH, Sheng JJ, Zhou WP, Ren J, Liu XD, Pan GY. Opposite regulation of hepatic breast cancer resistance protein in type 1 and 2 diabetes mellitus. European journal of pharmacology. 2014; 724:185–192. [PubMed: 24342797]

176. Maher JJ, Friedman SL. Parenchymal and nonparenchymal cell interactions in the liver. Seminars in liver disease. 1993; 13(1):13–20. [PubMed: 8446905]

177. Bale SS, Golberg I, Jindal R, McCarty WJ, Luitje M, Hegde M, Bhushan A, Usta OB, Yarmush ML. Long-term coculture strategies for primary hepatocytes and liver sinusoidal endothelial cells. Tissue Eng Part C Methods. 2015; 21(4):413–422. [PubMed: 25233394]

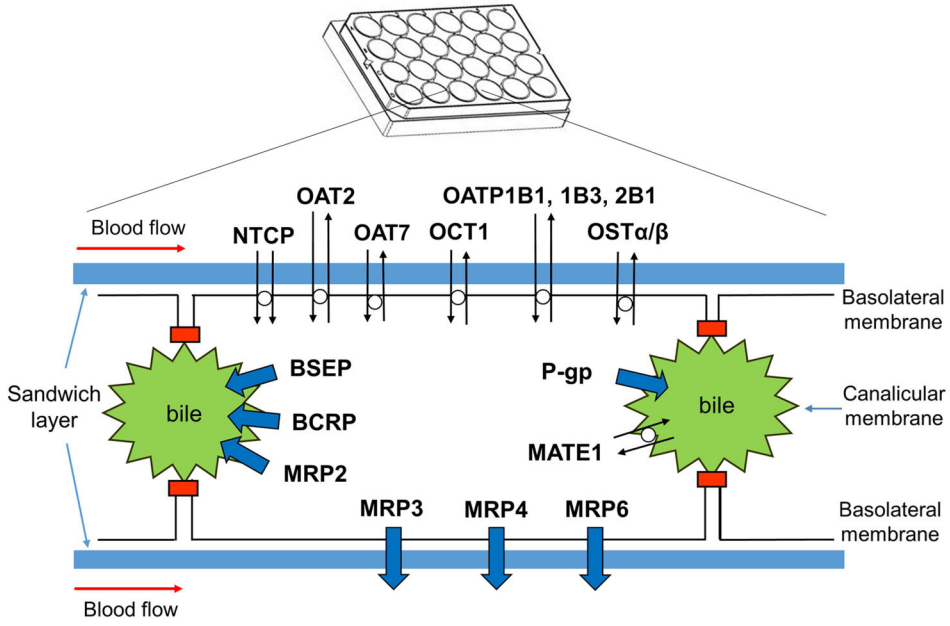

Figure 1. Scheme illustrating the polarized expression of transporters in human sandwich-cultured hepatocytes

Three adjacent hepatocytes with interconnecting canalicular spaces sealed by tight junctions are shown. Important ATP-binding cassette (ABC) transport proteins are depicted by blue solid arrows denoting the direction of transport. Solute carrier (SLC) transporters are depicted with black double arrows. Uptake transporters in the basolateral (sinusoidal) membrane include the sodium taurocholate co-transporting polypeptide (NTCP); organic anion transporter 2 (OAT2) and OAT7; organic cation transporter 1 (OCT1); and organic anion transporting polypeptide 1B1 (OATP1B1), OATP1B3 and OATP2B1. The heteromeric organic solute transporter (OSTα/β) is also depicted on the basolateral membrane. Efflux transporters expressed in the hepatocyte basolateral membrane include multidrug resistance-associated protein 3 (MRP3), MRP4 and MRP6. Canalicular (apical) efflux pumps include MRP2; breast cancer resistance protein (BCRP); bile-salt export pump (BSEP); MDR1 P-glycoprotein (Pgp); and multidrug and toxin extrusion protein 1 (MATE1).

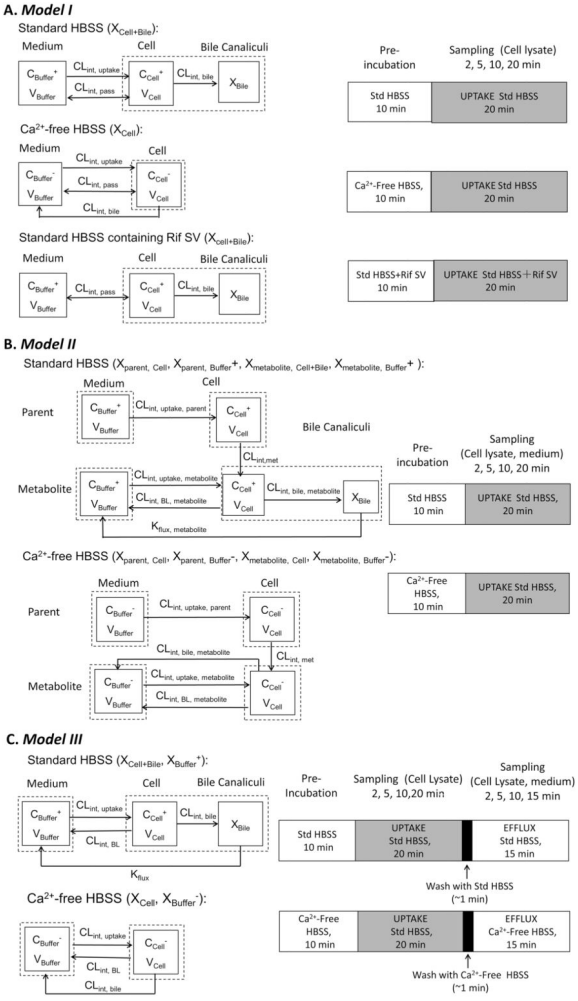

Figure 2. Schematic diagram depicting the mechanistic pharmacokinetic models (left) and experimental protocols (right) in SCH

(A) ***Model I,*** uptake studies were conducted in the presence of standard HBSS, Ca^{2+}-free HBSS, or standard HBSS containing rifamycin SV. **(B)** ***Model II,*** uptake studies were conducted in the presence of standard HBSS or Ca^{2+}-free HBSS. **(C)** ***Model III,*** uptake and efflux studies were conducted in the presence of standard HBSS or Ca^{2+}-free HBSS.

In the model schemes (left), dashed boxes represent the sampling compartments. X, V, and C denote the mass of substrate, compartmental volume, and substrate concentration, respectively. Subscripts on mass, bile and concentration terms denote the corresponding compartment in the model scheme, superscripts represent the presence and absence of Ca^{2+} in the pre-incubation and efflux buffer. X in parenthesis represents experimental measurements. Output parameters include: intrinsic uptake clearance ($CL_{int, uptake}$), intrinsic passive diffusion clearance ($CL_{int, pass}$), intrinsic biliary clearance ($CL_{int, bile}$), intrinsic metabolic clearance ($CL_{int, met}$), intrinsic basolateral efflux clearance ($CL_{int, BL}$), first-order rate constant for flux from bile networks into buffer (K_{flux}), intrinsic uptake clearance of parent ($CL_{int, uptake, parent}$), intrinsic uptake clearance of metabolite ($CL_{int, uptake, metabolite}$), intrinsic biliary clearance of metabolite ($CL_{int, bile, metabolite}$), intrinsic basolateral efflux

clearance of metabolite ($CL_{int, BL, metabolite}$), first-order rate constant for flux from bile networks into buffer of metabolite ($K_{flux, metabolite}$). In the experimental protocols diagram, the white boxes represent incubation with Ca^{2+}-free or standard HBSS. Grey shaded boxes represent inclusion of the substrate in standard HBSS during the uptake phase. Black boxes represent a 1-min wash with Ca^{2+}-free or standard HBSS. The sampling times and incubation length are shown in this diagram as an example, but need to be adjusted depending on the pharmacokinetic characteristics of the substrate.

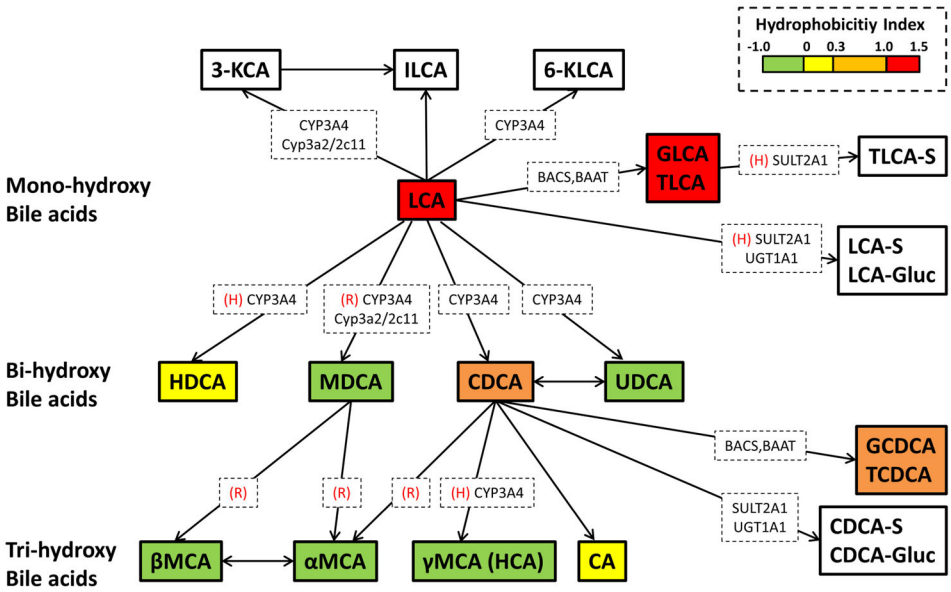

Figure 3. Hepatic metabolic pathways of lithocholic acid (LCA) and chenodeoxycholic acid (CDCA)

Schematic overview of previously reported metabolic pathways of LCA and CDCA in the liver. The hydrophobicity indices also are presented if the data were available from the literature. Conjugation pathways are only shown for LCA and CDCA, but other bile acids are also subject to glycine-, taurine-, sulfate-, or glucuronide-conjugation. (H) major pathway in humans; (R) major pathway in rats; 3-KCA, 3-ketocholic acid; 6-KLCA, 6-ketolithocholic acid; BAAT, bile acid:amino acid transferase; BACS, bile acid:coA synthase; CA, cholic acid; CDCA, chenodeoxycholic acid; CDCA-Gluc, chenodeoxycholic acid-glucuronide; CDCA-S, chenodeoxycholic acid-sulfate; CYP, cytochrome P450; GCDCA, glycochenodeoxycholic acid; GLCA, glycolithocholic acid; HCA, hyocholic acid; HDCA, hyodeoxycholic acid; ILCA, isolithocholic acid; LCA, lithocholic acid; LCA-Gluc, lithocholic acid-glucuronide; LCA-S, lithocholic acid-sulfate; αMCA, α-muricholic acid; βMCA, β-muricholic acid; γMCA, γ-muricholic acid; MDCA, murideoxycholic acid; SULT, sulfotransferase; TCDCA, taurochenodeoxycholic acid; TLCA, taurolithocholic acid; TLCA-S, taurolithocholic acid-sulfate; UDCA, ursodeoxycholic acid; UGT, UDP glucuronosyltransferase.

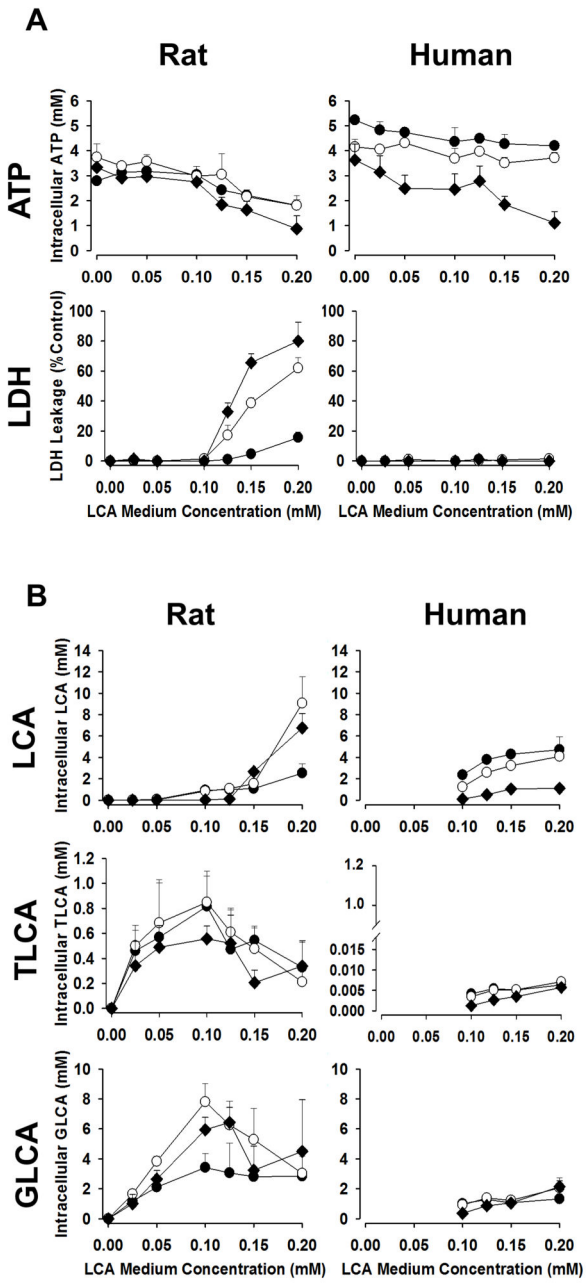

Figure 4. Toxicity and intracellular bile acid concentrations in lithocholic acid (LCA)-treated rat and human sandwich-cultured hepatocytes (SCH)

(A) Effects of LCA exposure on intracellular ATP and lactate dehydrogenase (LDH) release. Day 3 rat and day 6 human SCH were incubated with LCA (0–0.2mM) for 6hr (●), 12hr (●), and 24hr (◆). Representative data (mean±SD of triplicate determinations) from n=2 independent studies. **(B) Intracellular concentrations of LCA and LCA metabolites, glycolithocholic acid (GLCA) and taurolithocholic acid (TLCA).** Day 3 rat and day 6 human SCH were incubated with LCA (0–0.2mM) for 6hr (●), 12hr (○), and 24hr (◆). Intracellular LCA and LCA metabolites were measured by LC-MS/MS analysis of lysate after hepatocytes were incubated for 5min with Ca^{+2}-free HBSS buffer to open tight

junctions using B-CLEAR®.[114] Representative data (mean±SD of triplicate determinations) from n=1 (rat) or n=2 (human) independent studies.

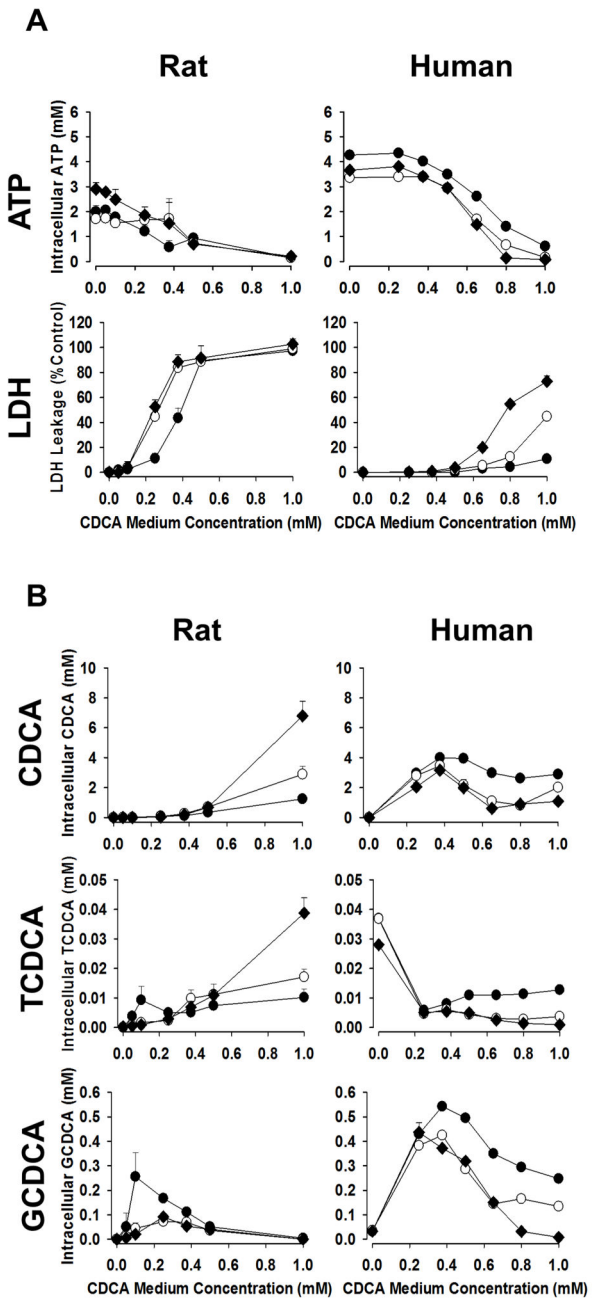

Figure 5. Toxicity and intracellular bile acid concentrations in chenodeoxycholic acid (CDCA)-treated rat and human sandwich-cultured hepatocytes (SCH)

(A) Effects of CDCA exposure on intracellular ATP and lactate dehydrogenase (LDH) release. Day 3 rat and day 6 human SCH were incubated with CDCA (0–1mM) for 6hr (●), 12hr (○), and 24hr (◆). Representative data (mean±SD of triplicate determinations) from n=2 independent studies. **(B) Intracellular concentrations of CDCA and CDCA metabolites, glycochenodeoxycholic acid (GCDCA) and taurochenodeoxycholic acid (TLCA).** Day 3 rat and day 6 human SCH were incubated with CDCA (0–1mM) for 6hr (●), 12hr (○), and 24hr (◆). Intracellular CDCA and CDCA metabolites were measured by

LC-MS/MS analysis of lysate after hepatocytes were incubated for 5min with Ca^{+2}-free HBSS buffer to open tight junctions using B-CLEAR®.[114] Representative data (mean±SD of triplicate determinations) from n=1 (rat) or n=2 (human) independent studies.

Table 1

Output parameters, assumptions, and applications of mechanistic pharmacokinetic modeling to assess clearance in SCH.

Type of Model	Output Parameters	Comments	Ref.
Model I	$CL_{int,\ uptake}$ $CL_{int,\ pass}$ $CL_{int,\ bile}$	**Assumptions:** • no basolateral efflux • no K_{flux} • $CL_{int,\ met}$ same as estimated from HLMs **Applications:** • substrates without basolateral efflux • $CL_{int,\ met}$ from other systems fixed in the model	60_62
Model II	$CL_{int,\ uptake,\ parent}$ $CL_{int,\ uptake,\ metabolite}$ $CL_{int,\ BL,\ metabolite}$ $CL_{int,\ bile,\ metabolite}$ $CL_{int,\ met}$ $K_{flux,\ metabolite}$	**Assumption:** • no passive diffusion • only metabolites effluxed into bile and medium **Applications:** • simultaneous estimation of transport clearance of parent and metabolite, as well as metabolic clearance	66 178 172
Model III	$CL_{int,\ uptake}$ $CL_{int,\ BL}$ $CL_{int,\ bile}$ K_{flux}	**Assumptions:** • no passive diffusion • no metabolism **Applications:** • accurate estimation of $CL_{int,\ BL}$ and K_{flux} by using a novel uptake and efflux protocol • useful for substrates minimally metabolized	6967,68

$CL_{int,\ uptake}$, intrinsic uptake clearance; $CL_{int,\ pass}$, intrinsic passive diffusion clearance; $CL_{int,\ bile}$, intrinsic biliary clearance; $CL_{int,\ met}$, intrinsic metabolic clearance; $CL_{int,\ BL}$, intrinsic basolateral efflux clearance; K_{flux}, first-order rate constant for flux from bile networks into buffer; $CL_{int,\ uptake,\ parent}$, intrinsic uptake clearance of parent; $CL_{int,\ uptake,\ metabolite}$, intrinsic uptake clearance of metabolite; $CL_{int,\ bile,\ metabolite}$, intrinsic biliary clearance of metabolite; $CL_{int,\ BL,\ metabolite}$, intrinsic basolateral efflux clearance of metabolite; $K_{flux,\ metabolite}$, first-order rate constant for flux from bile networks into buffer of metabolite; HLMs, human liver microsomes

Table 2

Medium and intracellular LCA or CDCA concentrations at the half-maximal toxicity after 24 hr incubation

Mean (95% confidence intervals) of the LCA or CDCA concentrations at the half maximal toxicity were estimated based on (A) medium concentrations and (B) intracellular bile acid concentrations by fitting a four parameter logistic model to the data obtained from *in vitro* rat and human sandwich-cultured hepatocytes. Parameters were not estimated for CDCA in human SCH because there was no direct relationship between intracellular CDCA and cytotoxicity.

Toxicity Measurement	LCA Rat SCH	LCA Human SCH	CDCA Rat SCH	CDCA Human SCH
(A) LC_{50} based on medium LCA or CDCA concentrations (mM)				
ATP	0.147 (0.132 – 0.164)	0.155 (0.136 – 0.178)	0.351 (0.292 – 0.422)	0.568 (0.532 – 0.607)
LDH	0.146 (0.140 – 0.152)	N.C.	0.243 (0.205 – 0.289)	0.972 (0.968 – 0.977)
(B) LC_{50} based on intracellular LCA or CDCA concentrations (mM)				
ATP	0.782 (0.314 – 1.95)	0.776 (0.485 – 1.24)	0.148 (0.0757 – 0.290)	N.C.
LDH	0.594 (0.250 – 1.41)	N.C	0.0371 (0.0114 – 0.121)	N.C.

N.C: not calculated.